IEEE Transactions on AUDIO

Volume AU-11 JULY-AUGUST, 1963 Number 4

Published Bimonthly

TABLE OF CONTENTS

PROFESSIONAL TECHNICAL GROUP ON AUDIO

IEEE TRANSACTIONS ON AUDIO

Published by The Institute of Electrical and Electronics Engineers, Inc., for the Professional Technical Group on Audio, at Box A, Lenox Hill Station, New York 21, N.Y. Responsibility for the contents rests upon the authors, and not upon the IEEE, the Group, or its members. Individual copies of this issue may be purchased at the following prices: IEEE members (one copy) $2.25, libraries and colleges $3.25, all others $4.50. Annual subscription price: nonmembers $17.00; colleges and public libraries $12.75.

Message from the New Chairman

Frank A. Comerci

THE MERGER of IRE with AIEE has now become a reality and the problems of merging the Professional Groups of the IRE with the Technical Operating Committees or Divisions of the AIEE have materialized as anticipated by our past chairman, Robert W. Benson. The organizational structures of the two societies are basically different and direct mergers are difficult. Also since many of the groups of one structure do not have a direct counterpart in the other structure, it is envisioned that the number of Professional Technical Groups which will emerge will be too large to permit adequate administration. Petitions for new Groups have already begun. In order to hold PTG's to a reasonable number, headquarters is urging that mergers be initiated as soon as possible. In cooperation with these desires and with the expectation that early merger will be to our future benefit, we have initiated discussions on merger with the PTG on Broadcasting. A meeting of the Administrative Committees of the two Groups has been arranged for the end of October to coincide with our Tutorial Session on Audio at the National Electronics Conference. In the event of such a merger I would expect that service to our membership would shift toward the industrial aspects of audio such as broadcasting, telephony and public address systems. Your comments are invited to assist in arriving at a decision which would best reflect your interests.

One of the major responsibilities of the AIEE TOC's was the formulation of Standards. Professional Groups have never had this responsibility. To facilitate mergers, the Professional Groups have now been given authority to proceed with Standards activities under coordination of the IEEE Standards Committee.

Your TRANSACTIONS *Editor*, Marvin Camras, has asked to be replaced. We have been fortunate in retaining his services over the last five years. I know we will all miss his humor in "The Editors Corner." I have hopes that we can induce him to carry on under a heading such as "The Exploits of Mr. Zilch," and perhaps even open this column to the members. Any of our humorously inclined members should send contributions to Peter Tappan, our new *Editor*, who is taking over these responsibilities starting with this issue.

Our technical meetings for this year will include the tutorial session previously mentioned with the NEC in Chicago on October 29th and I hope two sessions at the 1964 IEEE International Convention in the spring. Your officers are striving to continue with two meetings a year. The success of these meetings depends to a large extent on contributions from the group members. I would like to encourage these contributions especially from our younger engineers. Last year we were unable to make a "Junior Achievement Award" simply because there were no contributions from authors under age 30.

Our chapter's activity continues to be strong. I have been asked for assistance in promoting speakers and material for use in chapter meetings, and anticipate action to fulfill these requests.

I want to take this opportunity to thank all of you for the opportunity of serving you as Chairman of the Professional Technical Group on Audio. I am aware of the extreme responsibilities of the office in this critical period of merger and am in hopes that my contributions can help to make an even more effective group than exists as I take over the helm.

The Editor's Corner

Peter Tappan

HELLO

For the last five years, the editorial skill, clever humor and fond reminiscences of Marvin Camras have graced these pages. Having borne the burden overlong, he has at last cried "enough." It is now our turn to try to maintain the standards he has set.

We fear that we shall be able to surpass Marv's achievements in only one respect: tardiness. As you read this July-August issue, the snow may well be falling. We shall try to speed things up, though, and perhaps you will have the September-October issue by Christmas. Who knows? Some day the magazine may even come out on time!

For this to happen, we need your help in the form of good papers, letters, audio news and guest editorials; and we hope that some of these will be from Marvin Camras.

PTGA News

CHAPTER NEWS

A summary of the chapter activity for 1962–1963 as reported to Headquarters is as follows:

Boston

December 12, 1962: Daniel von Recklinghausen, H. H. Scott and Co., "Design Principles of Small, Wide Range, Direct-Radiator Loudspeaker Systems."

May 9, 1963: Joseph Kempler, Audio Devices, "Applications and Limitations of Joseph Kempler Magnetic Tape."

Chicago

September 11, 1962: Jack Mowry, B & K Instruments, "Precision Testing of Phonograph Sound Reproduction Components and Systems."

October 24, 1962: Robert Larson, Jensen Manufacturing Company, "The Jensen SUB-1 Underwater Loudspeaker."

December 14, 1963: Robert Larson, Jensen Manufacturing Company, "Loudspeaker Testing in Reverberant Rooms."

January 16, 1963: A. F. Petrie, General Electric Company, "G.E. Phono System Test Record."

May 29, 1963: Ladies Night at the Stage Light Theatre, Buffalo Grove, Ill.

Cincinnati

January 15, 1963: Albert Meyer, The Baldwin Piano Company, "Development of the Baldwin Three Manual Organ."

The Cincinnati Chapter PTGA provided the program for the final meeting of the Cincinnati IRE Section on June 10, 1963. The Cincinnati Section of IRE and AIEE merged on July 1 into the Cincinnati Section IEEE. This was a banquet meeting at which reminiscences of IRE Section activities over the years were followed by an audio demonstration lecture entitled "Music? of the Past, Present and Future." The speaker was Dr. D. W. Martin, Research Director of D. H. Baldwin Company (formerly Baldwin Piano). The demonstration material consisted of a variety of disc recordings, ranging chronologically from a 78 rpm recording of Lures (horns excavated in Northern Europe as bronze age relics) to the latest recordings available in electronic music composition and computer music. The principal point of the demonstration was that people like music of familiar types, and require time for adjustment to exotic types, whether new or old.

John Brean has served as Chairman of the Cincinnati Chapter of PTGA for the last two years, and will be succeeded by Thomas Cunningham for the coming year. Both men are engineers with the D. H. Baldwin Company.

Dayton

The Dayton Chapter of the Professional Technical Group on Audio featured two interesting and well attended meetings during the past year.

On November 7, 1962, the PTGA sponsored the Dayton Section meeting and arranged for Dr. Harry F. Olson of the RCA Laboratories to present an interesting topic, "Processing of Audio Information."

The presentation included a general description of the systems for the processing of audio information. This was followed by a specific and detailed description of the Electronic Music Synthesizer, the Random Probability System for composing music, the Phonetic Typewriter and the Syllable Communication System. There were demonstrations of music produced by the Electronic Music Synthesizer, of music composed by the Random Probability System and of speech transmitted by the Syllable Communication System.

The PTGA featured Stanley M. Slawsky of Smith Kline Precision, at their meeting at the Engineers' Club on December 5. Mr. Slawsky's interesting topic was "Ultrasonography in Medical Diagnosis." This lecture discussed research underway throughout the world on pulsed ultrasonic techniques in medical diagnosis. Typical design and clinical interpretation problems and findings were illustrated by examples drawn from the work of Dr. Gilbert Baum and the speaker in the field of ophthalmological diagnosis.

The new officers for the coming 1963–1964 year are Ray Kellogg, *Chairman*, A. Parker, *Vice Chairman*, and Ted Rynda, *Secretary*.

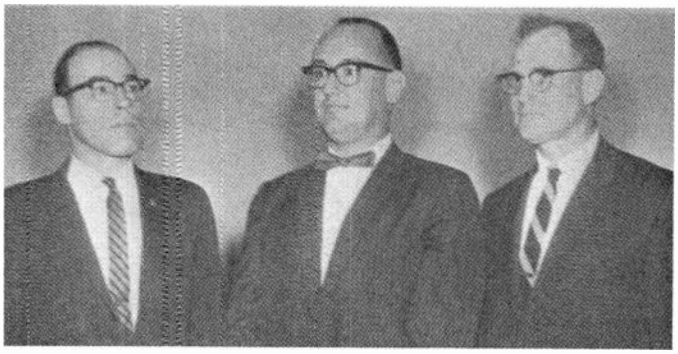

Left to right: T. Rynda, *Secretary*, R. Kellogg, *Chairman*, and A. Parker, *Vice Chairman*.

Minneapolis-St. Paul

December 11, 1962: Karl Kramer, Jensen Manufacturing Company, "Trends in Use and Design of Loudspeakers."

Philadelphia

November 16, 1962: Sidney Lidz, Dynaco Company, "FM Stereo Multiplex."

January 25, 1963: Lloyd Williams, Bolt, Beranek and Newman, Inc., and Leon Slawasky, General Sound Company, "Design Aspects of the Franklin Hall Sound Reinforcement System."

San Diego

June 4, 1963: L. B. Dalzell, Pacific Telephone Company, "Acoustical Feedback Stability Using Frequency Shift Techniques."

San Francisco

September 25, 1962: Myron Ferguson and Ralph Brown, Lenkurt Electronics Company, "Communication Satellite Problems and Solutions."

Washington, D. C.

December 4, 1962: Richard M. Siefkin, Delco Radio Division, General Motors Corp., "Engineering Considerations in the Design of an FM-AM Automobile Broadcast Receiver."

ANNOUNCEMENT

The PTGA is sponsoring a tutorial session at the National Electronics Conference, Chicago, Ill., on October 28, 1963. The program will be as follows:

1) "The State of the Art in Vocoder Techniques"—Dr. Edward E. David, Bell Telephone Laboratories, Murray Hill, N. J.
2) "Acoustical Analogies"—Benjamin Bauer, CBS Laboratories.
3) "Class B Audio Power Amplifiers"—Professor A. B. Bereskin, University of Cincinnati, Cincinnati, Ohio.
4) "Disk Records, A Review and Evaluation"—Dr. Abraham M. Max, Radio Corporation of America, Camden, N. J.
5) "Magnetic Recording"—Marvin Camras, Armour Research Foundation, Illinois Institute of Technology, Chicago, Ill.

An Analysis of the Magnetic Circuit of Multitrack Record and Playback Heads*

C. B. SPEEDY†

Summary—An analysis is given of the magnetic circuit of a recording (or playback) head in a multitrack assembly. In particular the analysis is concerned with the effect of leakage flux between the core of the head and the closely spaced screen which separates neighboring heads in the assembly. The analysis includes the reluctance of the front and rear gaps, and also the distributed nature of the core and leakage path reluctances. Expressions are derived for sensitivity and inductance in terms of three dimensionless parameters which refer to core, leakage and rear gap reluctances, respectively. Graphical results are included for typical values of the parameters.

List of Principal Symbols

The rationalized mks system of units is used throughout the paper.

ϕ = Magnetic flux
F = Magnetomotive force
μ = Permeability of core
μ_0 = Permeability of space
$\mu_c = \mu/\mu_0$
U = Normalized core reluctance
H = Normalized leakage reluctance
A = Normalized back gap reluctance
R = Reluctance
r = Reluctance of core per unit length of core
s = Permeance of leakage path per unit length of core
$k = \sqrt{rs}$
I = Current in head winding
N = Number of turns in head winding
z = Flux linkages
S = Sensitivity of head
L = Inductance of head
w = Length of core
p = Width of core
c = Thickness of core
n = Depth of front gap
h = Depth of back gap
d = Length of both front and back gaps
v = Screen separation.

I. Introduction

A MAGNETIC RECORDING HEAD comprises essentially a magnetic circuit of low reluctance with a gap at the point where the head comes in contact with, or in close proximity to, the magnetic recording medium. During recording, the magnetomotive force produced by the current in the winding appears largely across this gap and causes a small element of the medium to be magnetized. When such an element is subsequently moved across the gap of a playback head a portion of the flux from the element links with the head winding and causes a voltage to be induced. In perfect heads, the full winding magnetomotive force would appear across the front gap during recording, and the total flux from the element would link with all turns of the winding on playback. In practice this ideal is not realized, and it is the purpose of this study to examine the factors which influence the efficiency of these processes.

In a single isolated head of suitable proportions, the flux is confined mainly to the iron circuit, and the leakage flux is comparatively small. With a multitrack arrangement in which heads are of necessity placed close to each other, it becomes important to introduce screens between heads to reduce the magnetic coupling which would otherwise be quite severe. The screens thus by their very nature provide shunt paths for leakage flux and disturb the performance of the heads themselves. It is this situation, in which a head is located between two closely spaced screens, that is the subject of the following analysis.

In a head with modest core permeability, a portion of the flux flows in the core and the remainder in the leakage path which includes the screens. This leakage flux emanates not from a point on the core but rather from the whole surface of the core, and in particular, from the surface adjacent to the screen. In the present analysis the distributed nature of the leakage flux path is taken into consideration, although certain simplifying assumptions are made about the geometry of the head and of the flux paths themselves in order to facilitate the analysis.

The first step in the analysis is to establish the general equations for the magnetomotive force and flux in the head. From the general equations, boundary conditions existing at both front and back gaps are introduced, and expressions derived for the sensitivity (or efficiency) of both record and playback heads, and for the inductance of record heads. These expressions are rearranged in terms of three dimensionless parameters, U, H and A, which refer, respectively, to the ratio of the reluctance of the core, leakage path and back gap respectively to that of the front gap. Values of sensitivity and inductance are tabulated for a typical range of the parameters, and presented in graphical form.

* Received April 25, 1963.
† University of New South Wales, New South Wales, Australia.

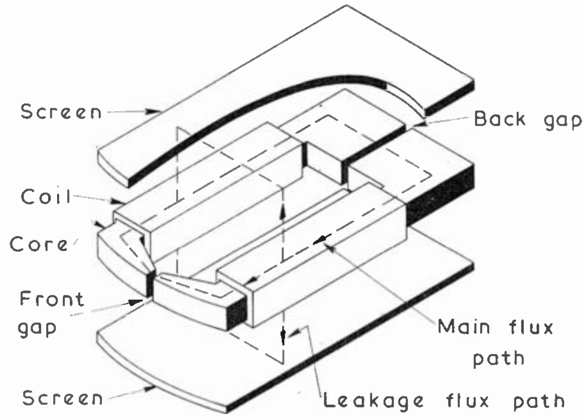

Fig. 1—Head located between screens.

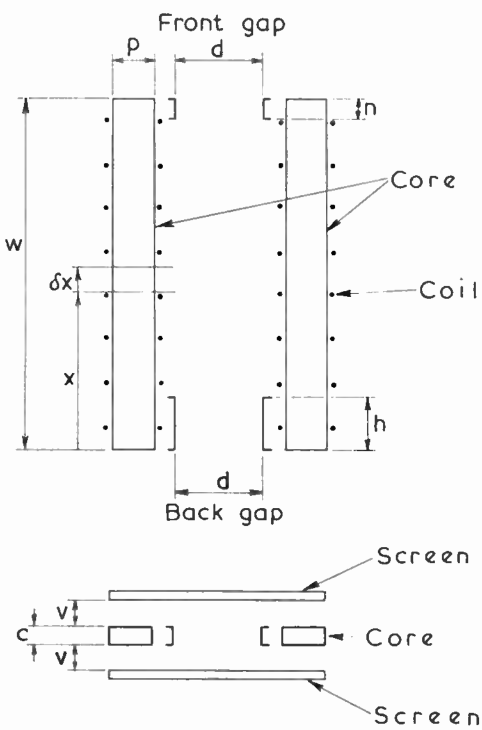

Fig. 2—Head dimensions.

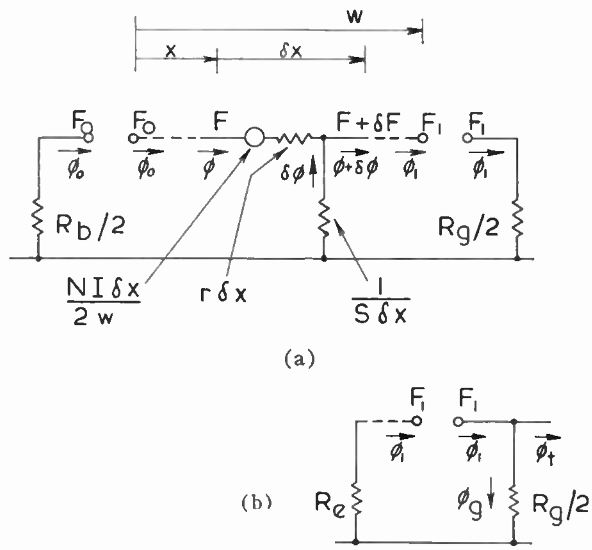

Fig. 3—Reluctance circuits. (a) Record head. (b) Playback head.

II. Magnetic Circuit

The type of magnetic head to which the present study applies is shown in Fig. 1. It comprises the head itself located between two closely spaced magnetic screens. The main flux passes through the two legs of the core and the front and back gaps whereas the leakage flux passes from one leg of the core to the other through the screens. Leakage flux occurs at all points on the surface of the core.

For analysis, it is assumed that each leg of the core is of simple rectangular shape as indicated in Fig. 2. Each half of the winding is assumed to be uniformly distributed along the full length of each leg. Since the two gaps in the main flux path are short compared with their width, fringing fields at the edges of the gaps are neglected and the flux paths across the gaps assumed to be perpendicular to the pole faces. Similarly the leakage flux is assumed to flow normally between adjacent parallel surfaces of the core and screens, fringing effects being neglected.

By symmetry, the plane which bisects the front and back gaps and which is normal to the plane of the screens is a plane of zero magnetic potential. Therefore, in the analysis all magnetic potentials are referred to the zero potential on this plane. The equivalent reluctance circuit for one leg is indicated in Fig. 3(a).

By reluctance of an element of length δx of one leg of the core is given by

$$r\delta x = \frac{\delta x}{\mu p c}. \tag{1}$$

The permeance of the leakage path associated with an element of one leg of core of length δx (noting that there are two parallel paths; one to each screen), is

$$s\delta x = \frac{2\mu_0 p \delta x}{v}. \tag{2}$$

The change in magnetomotive force across the elements is

$$\delta F = -\phi r \delta x + \frac{NI\delta x}{2w}. \tag{3}$$

The change in flux in the element is

$$\delta\phi = -Fs\delta x$$

$$\therefore \frac{d^2F}{dx^2} = -r\frac{d\phi}{dx} = Frs \tag{4}$$

and

$$\frac{d^2\phi}{dx^2} = -s\frac{dF}{dx} = \phi rs - \frac{NIs}{2w}. \tag{5}$$

The general solution of (4) is

$$F = Ae^{kx} + Be^{-kx} \tag{6}$$

where

$$k^2 = rs. \tag{7}$$

Let $F=F_0$ when $x=0$ and $F=F_1$ when $x=w$. Substituting these in (6) and eliminating A and B,

$$F = \frac{F_0 \sinh k(w-x)}{\sinh kw} + \frac{F_1 \sinh kx}{\sinh kw}. \tag{8}$$

From (5),

$$\phi = \frac{NI}{2wr} + \frac{F_0 k \cosh k(w-x)}{r \sinh kw} - \frac{F_1 k \cosh kx}{r \sinh kw}. \tag{9}$$

$$S_R = \frac{\dfrac{kw}{\sinh kw} - \left(\dfrac{kw \cosh kw}{\sinh kw} + \dfrac{rw}{R_b/2}\right)}{\dfrac{k^2w^2}{\sinh^2 kw} - \left(\dfrac{kw \cosh kw}{\sinh kw} + \dfrac{rw}{R_g/2}\right)\left(\dfrac{kw \cosh kw}{\sinh kw} + \dfrac{rw}{R_b/2}\right)}. \tag{17}$$

Let $\phi=\phi_0$ when $x=0$ and $\phi=\phi_1$ when $x=w$,

$$\therefore \phi_0 = \frac{NI}{2wr} + \frac{F_0 k \cosh kw}{r \sinh kw} - \frac{F_1 k}{r \sinh kw} \tag{10}$$

and

$$\phi_1 = \frac{NI}{2wr} + \frac{F_0 k}{r \sinh kw} - \frac{F_1 k \cosh kw}{r \sinh kw}. \tag{11}$$

III. Record Head Sensitivity

To determine the magnetomotive force at the front gap resulting from the winding current consider first the boundary conditions. At

$$x = 0, \qquad \phi_0 = -\frac{F_0}{R_b/2} \tag{12}$$

and at

$$x = w, \qquad \phi_1 = \frac{F_1}{R_g/2} \tag{13}$$

where

$$R_b = \frac{d}{\mu_0 hc} \tag{14}$$

and

$$R_g = \frac{d}{\mu_0 nc}. \tag{15}$$

Since the magnetomotive force across the front gap is $2F_1$, let the sensitivity of the record head be defined by

$$S_R = \frac{2F_1}{NI}. \tag{16}$$

From (10) and (12)

$$0 = \frac{NI}{2wr} + F_0\left(\frac{k \cosh kw}{r \sinh kw} + \frac{1}{R_b/2}\right) - \frac{F_1 k}{r \sinh kw}$$

and from (11) and (13)

$$0 = \frac{NI}{2wr} + \frac{F_0 k}{r \sinh kw} - F_1\left(\frac{k \cosh kw}{r \sinh kw} + \frac{1}{R_g/2}\right).$$

Eliminating F_0 from these two equations and rearranging according to (16)

To express the sensitivity in nondimensional terms let

$$U = \frac{\text{reluctance of the iron circuit}}{\text{reluctance of the front gap}} = \frac{2rw}{R_g} = \frac{2nw}{\mu_c pd}. \tag{18}$$

Let the reluctance of the leakage path be expressed in terms of

$$H = \frac{\text{reluctance of total leakage path}}{\text{reluctance of the front gap}} = \frac{cvn}{wpd}. \tag{19}$$

Let the reluctance of the back gap be referred to that of the front gap by

$$A = \frac{\text{reluctance of back gap}}{\text{reluctance of front gap}} = \frac{n}{h}. \tag{20}$$

For convenience the term kw may be retained in the expressions for sensitivity where

$$k^2w^2 = \frac{U}{H}. \tag{21}$$

From (17), S_R expressed in terms of U, H, A and kw is

$$S_R = \frac{\dfrac{kw(\cosh kw - 1)}{\sinh kw} + \dfrac{U}{A}}{k^2w^2 + \dfrac{kw \cosh kw}{\sinh kw}\left(U + \dfrac{U}{A}\right) + \dfrac{U^2}{A}}. \tag{22}$$

The limiting value when $\mu_c \to 0$ ($kw \to \infty$, $U \to \infty$)

$$S_{R,0} = \frac{1}{U}. \tag{23}$$

The limiting value when $\mu_c \to \infty$ ($kw \to 0$, $U \to 0$)

$$S_{R,\infty} = \frac{\dfrac{A}{2} + H}{A + AH + H}. \tag{24}$$

IV. Playback Head Sensitivity

During the replay process in which magnetized tape moves across the playback head, flux from the tape links with the winding of the head. A recluctance circuit diagram is shown in Fig. 3(b).

The flux ϕ_t from a magnetized portion of the tape enters the pole tip and divides into ϕ_g which passes across the front gap, and ϕ_1 which enters the main circuit.

$$\phi_t = \phi_1 - \phi_g. \tag{25}$$

Since the reluctance of the element of tape across the front gap is in practice generally much greater than that of either the front gap or the main circuit, the flux ϕ_t is not significantly influenced by the actual value of the reluctance of the playback head. It is assumed in the present analysis that ϕ_t is independent of the playback head reluctance.

Inspection of Fig. 3(b) shows that the magnetomotive force and flux are given by the same equations as for the record head, namely (3) and (4), respectively, except that in the present case the current is zero. It follows that (5)–(11) inclusive, with $I=0$, apply equally to the playback head.

In the playback head let the equivalent reluctance of one leg of the core (excluding the shunt effect of the front gap) be denoted by R_e where

$$R_e = \frac{-F_1}{\phi_1}. \tag{26}$$

From (25) and (26)

$$\frac{\phi_1}{\phi_t} = \frac{R_g/2}{R_g/2 + R_e}. \tag{27}$$

From Fig. 3(b) when $x=0$,

$$\phi_0 = \frac{-F_0}{R_b/2}. \tag{28}$$

From (10) and (28) when $I=0$,

$$0 = F_0\left(\frac{k \cosh kw}{r \sinh kw} + \frac{1}{R_b/2}\right) - \frac{F_1 k}{r \sinh kw}.$$

Eq. (11), when $I=0$,

$$\phi_1 = \frac{F_0 k}{r \sinh kw} - \frac{F_1 k \cosh kw}{r \sinh kw}.$$

Eliminating F_0 from these two equations and substituting in (26),

$$\frac{R_e}{rw} = \frac{\cosh kw + \dfrac{2rw}{R_b}\dfrac{\sinh kw}{kw}}{kw \sinh kw + \dfrac{2rw}{R_b}\cosh kw}. \tag{29}$$

From (9) and (26) when $I=0$,

$$\phi = \frac{F_0 k \cosh k(w-x)}{r \sinh kw} + \frac{\phi_1 R_e k \cosh kw}{r \sinh kw}. \tag{30}$$

From (11) and (26) when $I=0$,

$$\phi_1 = \frac{F_0 k}{r \sinh kw} + \frac{\phi_1 R_e k \cosh kw}{r \sinh kw}. \tag{31}$$

From these two equations,

$$\phi = \phi_1\left(\left(1 - \frac{R_e k \cosh kw}{r \sinh kw}\right)\cosh k(w-x) + \frac{R_e k \cosh kw}{r \sinh kw}\right). \tag{32}$$

The resultant flux linkages with the windings are given by

$$z = \frac{N}{w}\int_0^w \phi\, dx. \tag{33}$$

From (32) and (33),

$$z = N\phi_1\left(\left(1 - \frac{R_e k \cosh kw}{r \sinh kw}\right)\frac{\sinh kw}{kw} + \frac{R_e}{rw}\right). \tag{34}$$

In the ideal playback head, all the flux from the tape links with all turns of the winding. Therefore let the sensitivity of the playback head be denoted by S_P where

$$S_P = \frac{z}{\phi_t N}. \tag{35}$$

From these two equations,

$$F_1 = \frac{\dfrac{NI}{2wr}\left(\dfrac{k}{r\sinh kw} - \dfrac{k\cosh kw}{r\sinh kw} - \dfrac{1}{R_b/2}\right)}{\dfrac{k^2}{r^2\sinh^2 kw} - \left(\dfrac{k\cosh kw}{r\sinh kw} + \dfrac{1}{R_b/2}\right)\left(\dfrac{k\cosh kw}{r\sinh kw} + \dfrac{1}{R_g/2}\right)} \tag{39}$$

and

$$F_0 = \frac{\dfrac{NI}{2wr}\left(\dfrac{k\cosh kw}{r\sinh kw} + \dfrac{1}{R_g/2} - \dfrac{k}{r\sinh kw}\right)}{\dfrac{k^2}{r^2\sinh^2 kw} - \left(\dfrac{k\cosh kw}{r\sinh kw} + \dfrac{1}{R_b/2}\right)\left(\dfrac{k\cosh kw}{r\sinh kw} + \dfrac{1}{R_g/2}\right)}. \tag{40}$$

From (27), (29), (34), (35) and (18), (19) and (20),

$$S_P = \frac{\dfrac{kw(\cosh kw - 1)}{\sinh kw} + \dfrac{U}{A}}{k^2w^2 + \dfrac{kw\cosh kw}{\sinh kw}\left(U + \dfrac{U}{A}\right) + \dfrac{U^2}{A}}, \tag{36}$$

where $k^2w^2 = U/H$; this equation is the same as (22) and hence the limiting conditions are as given by (23) and (24). The limiting value when $\mu_c \rightarrow 0 (kw \rightarrow \infty,\ U \rightarrow \infty)$

$$S_{P,0} = \frac{1}{U}. \tag{37}$$

The limiting value when $\mu_c \rightarrow \infty$ $(kw \rightarrow 0,\ U \rightarrow 0)$

$$S_{P,\infty} = \frac{\dfrac{A}{2} + H}{A + AH + H}. \tag{38}$$

V. Record Head Inductance

The method used to derive the record head inductance is to establish the flux distribution arising from a given winding current, and to determine the subsequent flux linkages with the winding. From (10) and (12),

$$0 = \frac{NI}{2wr} + F_0\left(\frac{k\cosh kw}{r\sinh kw} + \frac{1}{R_b/2}\right) - \frac{F_1 k}{r\sinh kw}.$$

From (11) and (13),

$$0 = \frac{NI}{2wr} + \frac{F_0 k}{r\sinh kw} - F_1\left(\frac{k\cosh kw}{r\sinh kw} + \frac{1}{R_b/2}\right).$$

From (9) and (33), the flux linkages are given by

$$z = \frac{N}{rw}\left(\frac{NI}{2} + F_0 - F_1\right) \tag{41}$$

where F_0 and F_1 are given by (40) and (39). Let the inductance of the head be denoted by

$$L = \frac{z}{I}. \tag{42}$$

Let a normalized value of inductance be

$$L_R = \frac{LR_g}{N^2} = \frac{zR_g}{IN^2}. \tag{43}$$

Substituting (39), (40) and (41) in (43),

$$L_R = \frac{R_g}{2rw}\left[1 + \frac{\dfrac{2kw\cosh kw}{\sinh kw} + \dfrac{rw}{R_g/2} + \dfrac{rw}{R_b/2} - \dfrac{2kw}{\sinh kw}}{\dfrac{k^2w^2}{\sinh^2 kw} - \left(\dfrac{kw\cosh kw}{\sinh kw} + \dfrac{rw}{R_b/2}\right)\left(\dfrac{kw\cosh kw}{\sinh kw} + \dfrac{rw}{R_g/2}\right)}\right]. \tag{44}$$

Expressed in terms of U, H, A and kw,

$$L_R = \frac{1}{U}\left[1 - \frac{\dfrac{2kw(\cosh kw - 1)}{\sinh kw} + U + \dfrac{U}{A}}{k^2w^2 + \dfrac{kw\cosh kw}{\sinh kw}\left(U + \dfrac{U}{A}\right) + \dfrac{U^2}{A}}\right] \tag{45}$$

where $k^2w^2 = U/H$.

The limiting value when $\mu_c \rightarrow 0 (kw \rightarrow \infty,\ U \rightarrow \infty)$

$$L_{R,\infty} = \frac{1}{U}. \tag{46}$$

The limiting value when $\mu_c \rightarrow \infty$ $(kw \rightarrow 0,\ U \rightarrow 0)$

$$L_{R,0} = \frac{\frac{1}{2}(A+1) + H}{A + AH + H}. \tag{47}$$

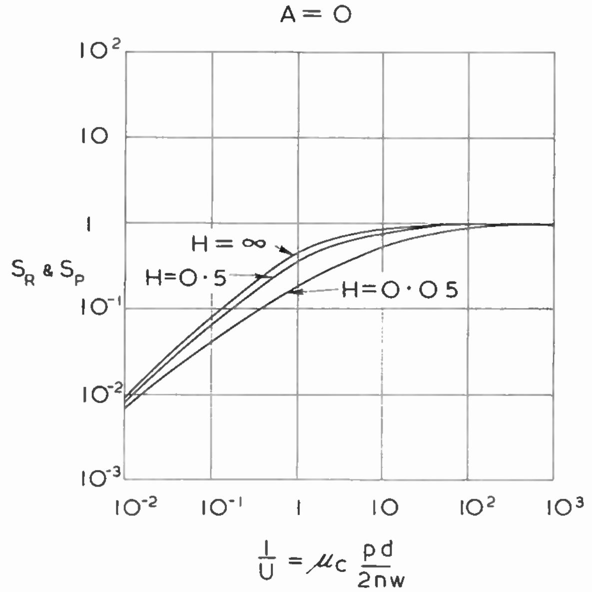

Fig. 4—Head sensitivity ($A=0$).

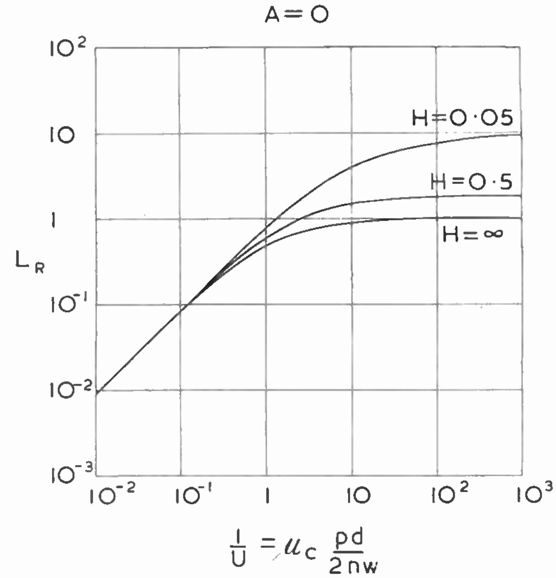

Fig. 6—Record head inductance ($A=0$).

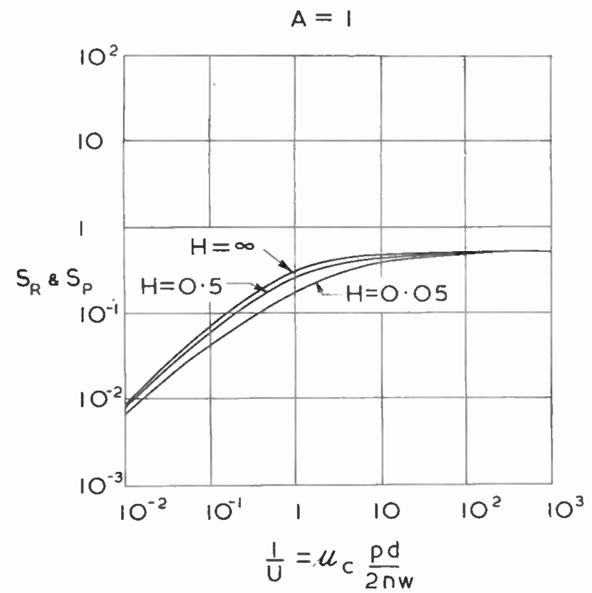

Fig. 5—Head sensitivity ($A=1$).

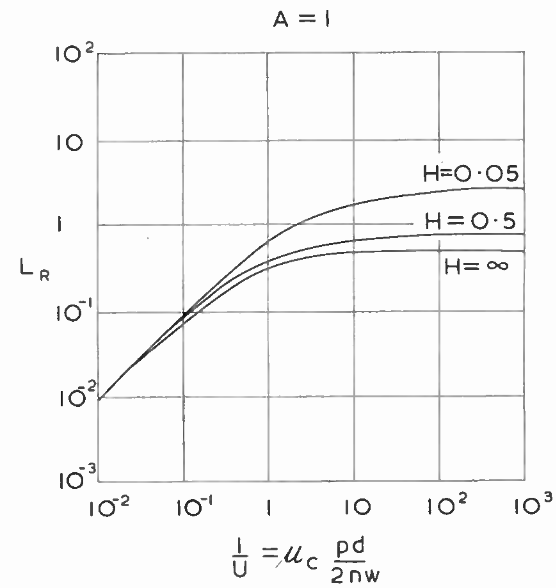

Fig. 7—Record head inductance ($A=1$).

VI. Conclusion

The magnetic circuit of a recording head with its two adjacent screens is analyzed, and the results expressed in terms of three meaningful parameters. One of these denotes the core reluctance, the second the leakage reluctance, and the third refers to the rear gap reluctance. Due consideration is given to the distributed nature of both the core and leakage reluctance. Certain preliminary assumptions regarding the general shape of the magnetic field problem are made, which are appropriate to heads of conventional dimensions. Should the theoretical results be applied out of this context, due consideration would need to be given to errors arising from these approximations.

Head sensitivity is shown to depend upon core, leakage and rear gap reluctances. To a first approximation it is shown that for cases where the core reluctance is considerably less than front gap reluctance, sensitivity is substantially constant and dependent only upon rear gap reluctance. When the core reluctance is appreciably higher than that of the front gap the sensitivity is dependent only upon the core reluctance to which it is approximately inversely proportional. In the middle range where the core reluctance is of the same order as that of the front gap, the sensitivity is lowered by both rear gap reluctance and the presence of leakage reluctance.

In a generally similar manner, inductance is closely related to core reluctance. When the core reluctance is considerably higher than that of the front gap, the inductance is low and is approximately inversely proportional to the core reluctance. For very low values of core reluctance, the inductance is dependent upon the reluctances of the rear gap and leakage path. The effect of the former is to lower the inductance in this region, and that of the latter is to increase the inductance. Formulas are derived for these limiting cases which show this relationship in detail. In the middle range where core and front gap reluctance are of the same order, inductance is dependent upon all three parameters. It is lowered by increasing the core reluctance, by increasing the rear gap reluctance, or by increasing the leakage reluctance.

The equations, which have been derived in terms of head dimensions, show the effect of core, leakage and rear gap reluctance upon both head sensitivity and inductance. Within the limits of the simplifying assumption used in the analysis the results provide a comprehensive basis for the design of the magnetic circuit of multitrack record and playback heads.

VII. References

[1] A. S. Hoagland, "Magnetic data recording theory: head design," *AIEE Trans.* vol. 75 (*Communications and Electronics*), pp. 506–512; November, 1956.

[2] K. Singer and M. Rettinger, "Multiple-track magnetic head," *SMPTE*, vol. 61, pp. 390–394; September, 1953.

[3] S. Duinker, "Durable high-resolution, transducer heads employing bonding glass spacers," *Philips Res. Repts.*, vol. 15, pp. 352–367; 1960.

[4] D. F. Eldridge and A. Baaba, "The effect of track width in magnetic recording," IRE Trans. on Audio, vol. AU-9, pp. 10–14; January–February, 1961.

Design and Fabrication of a Prototype Speech Synthesizer*

H. ITO† and D. G. BURKHARD†

Summary—Speech synthesizing circuitry for use with hand-painted spectra is described.

Photocontrolled audio oscillators are employed to obtain pure tones. Oscillation conditions are examined in a unified form for both vacuum tube and transistor circuitry. Amplitude stabilization is discussed employing a complex load.

A prototype unit with six oscillators is found to have excellent frequency and amplitude stability for arbitrary audio oscillator frequencies. With additional oscillators, photo diode control of the sound intensity will provide the necessary flexibility for speech synthesis.

Introduction

When a speech sound is Fourier analyzed, it is found to consist of a fundamental frequency and its harmonics. The fundamental frequency and relative amplitudes of the harmonics will characterize a single sustained sound. The fundamental frequency and harmonic composition will vary, of course, from sound to sound. In forming words or even in the sounding of vowels and consonants, it is found that a continuous shift of the fundamental and its harmonics takes place while the word or vowel is articulated.

In order to synthesize speech, it is necessary to reverse the above process and to form fundamentals plus harmonics whose amplitudes are time dependent. The characteristic ways in which such time dependent amplitude factors enter the formation of units of speech are called formants. The characteristics of these formants have been studied in detail by many investigators including P. Delattre.[1]

A procedure for electronically synthesizing the critical formants in order to create artificial speech has been described by F. S. Cooper and by J. M. Borst.[2] The instrument is discussed in detail in both of the papers.[2] A schematic of the apparatus is shown in Fig. 1. A light source provides an intense thin line of light which is focused radially on a rotating disk. This "tone wheel" is a film negative which carries 50 concentric variable density sound tracks. The inner one has four sine waves on it, the next one, 2×4 sine waves, the next one, 3×4 sine waves, etc. By rotating the disk at 1800 rpm, by a synchronous motor, the tone wheel will yield a modulated light signal at 120 cps intervals from 120 cps to 6000 cps.

The modulated line of light is focused on the moving spectrogram which consists of light and dark areas on a plastic film. The film is transported by two rotating drums. The light and dark areas then continuously pass and intercept the line of light being directed on the photocell. If this is an original spectrogram (photographic negative), the instrument is used with the phototube placed below the rotating film so that the light

* Received August 28, 1962; revised manuscript received April 12, 1963.

† Department of Physics, University of Colorado, Boulder, Colo.

[1] P. Delattre, "Les indices acoustiques de la parole," *Phonetica*, vol. 2, pp. 108–118, 226–251; 1958.

[2] J. M. Borst, "The use of spectrograms for speech analysis and synthesis," *J. Audio Engrg. Soc.*, vol. 4, pp. 14–23; 1956.

F. S. Cooper, "Some Instrumental Aids to Research on Speech," Rept. on 4th Annual Round Table Meeting on Linguistics and Language Teaching 46-53; September, 1953.

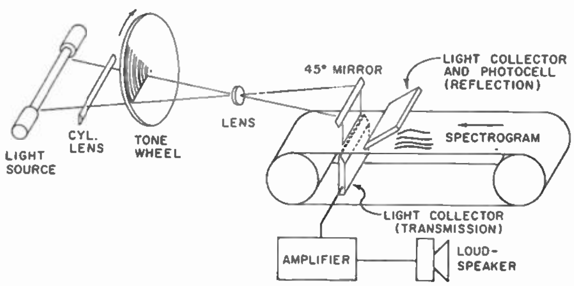

Fig. 1—Schematic diagram of tone wheel speech synthesizer (Cooper and Borst[2]).

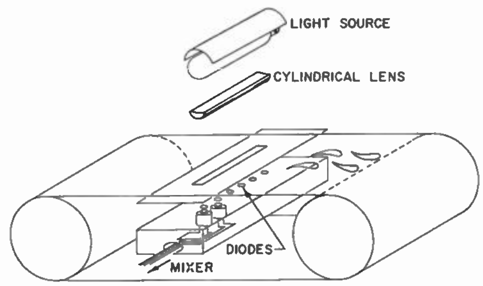

Fig. 2—Schematic diagram of phototransistor speech synthesizer.

which passes through will be collected. In synthesizing speech an artificial or hand-painted spectrogram is employed, so that a reflection system is used and the light collector is then placed above the spectrogram. Wherever there is white paint on the transparent tape, light will be diffusely reflected into the collector. The light is modulated at a frequency determined by its position along the transverse or frequency axes of the spectrogram.

The frequencies are limited to those which have been placed on the "tone wheel" and, in this particular instrument, are harmonically related starting from a fundamental of 120 cps. The instrument therefore is not so flexible as one might desire. For example, one may wish to change the absolute frequencies, and also to study the role of harmonic relation in synthesizing human speech.

In order to create a more flexible unit and still employ the powerful technique of the hand-painted spectrogram, one may discard the tone wheel and replace the single photocell by an arbitrary number (say 50) of individually photocontrolled oscillators. The oscillators will be in off position when exposed to a light beam. Oscillation begins when the light beam is interrupted, that is, when the beam is prevented from reaching the control photodiodes. A schematic of this design is shown in Fig. 2. In this case the amplitude variation with time of the various frequencies is formed by drawing opaque "formants" on the rotating transparent tape. In this type of design, it would be possible to vary the frequencies of the "harmonics," but in our experiments we wished to vary the amplitudes of the harmonics in a systematic way by quantitatively controlling the amount of light transmitted to the diodes. This can be done by using standard parallel lines parallel to the direction of motion of the drum in sketching the formants.

Block Diagram

A block diagram of the system is shown in Fig. 3. In the present prototype system six pure tone variable oscillators were built on a single chassis. Six tones are not sufficient in number to synthesize speech, but they have proven sufficient to illustrate some vowel characteristics. Oscillator output is controlled by the photodiode circuit, which in turn is regulated by the light beam transmitted by the rotating tape. Photodiode circuit output signal is amplified by means of a standard audio amplifier before entering the loud speaker.

We now briefly describe the oscillator and photodiode circuit.[3]

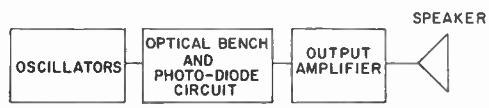

Fig. 3—Block diagram of phototransistor speech synthesizer.

RC Oscillator

Among the many possible oscillator circuits, the RC oscillator or so-called Wien bridge oscillator is used because of its stability and small distortion content. Vacuum tube circuitry has been employed in our present model. For size minimization and for less power dissipation a transistorized circuit would be preferable. A bank of transistorized oscillators has been constructed for the present application, but the over-all stability of the unit was not so high as that of the vacuum tube circuit. Improvement of the transistorized circuit is possible, however. In order that the design procedure may be applicable to either a vacuum tube or transistor circuit we present a general circuit analysis of the oscillator circuit. The following discussion is an extension of the treatment of M. A. Melehy.[4]

The essentials of the oscillator circuit are shown in Fig. 4(a). The amplifier may consist of a vacuum tube or transistor or circuits of either. One may define the following characteristics for the amplifier:

Z_{in}: input impedance

Z_{out}: output impedance

A_i: current amplification factor.

The input impedance as seen from the point b is

$$Z_b = R_b + Z_{in}. \tag{1}$$

[3] More detailed circuit analysis is contained in H. Ito, "A Prototype Speech Synthesizer," M.S. thesis, University of Colorado, Boulder; 1962.

[4] M. A. Melehy, "A wide-range junction transistor audio oscillator," 1958 IRE WESCON Convention Record, pt. 2, pp. 74–77.

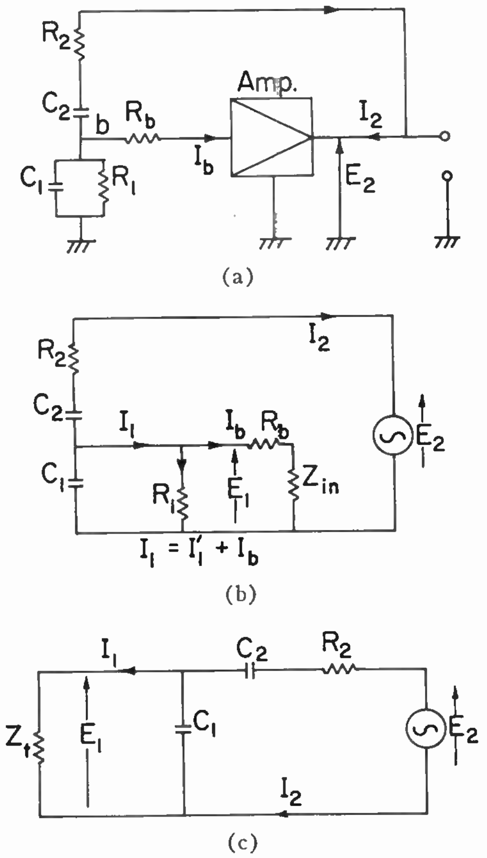

Fig. 4—Actual and equivalent circuit diagram of RC-oscillator. (a) Actual circuit diagram where amplifier is represented by "Amp." (b) and (c) Equivalent circuit.

In the audio frequency range Z_b may be written

$$Z_b = R_b \text{ for transistor } (R_b \gg Z_{in})$$

$$Z_b = Z_{in} \text{ for vacuum tube } (R_b \ll Z_{in}).$$

If the following condition holds for the output impedance of the amplifier

$$|Z_{out}| \ll \left\{\left[R_2 + \frac{R_1}{M}\left\{(R_b + R_{in})(R_1 + R_b + R_{in}) + \frac{1}{\omega^2 C_{in}{}^2}\right\}\right]^2 + \left[\left(\frac{1}{\omega C_2}\right) + \frac{R_1{}^2}{M}\left\{\omega C_1 (R_b + R_{in})^2 + \frac{1}{\omega C_{in}}\left(1 + \frac{C_1}{C_{in}}\right)\right\}\right]^2\right\}^{1/2} \quad (3)$$

where we have used

$$Z_{in} = R_{in} + 1/j\omega C_{in}$$

and

$$M = [R_1(1 + C_1/C_{in}) + R_b + R_{in}]^2 + \left[\omega C_1 R_1 (R_b + R_{in}) - \frac{1}{\omega C_{in}}\right]^2,$$

then the circuit in the Fig. 4(a) may be reduced to the circuit of Fig. 4(b). E_2 is the output voltage of the oscillator circuit. It is an active element in the equivalent circuit Fig. 4(b), and is the voltage supplied by the amplifier.

Referring to Fig. 4(b) one has

$$E_2 = I_2 Z_{out}$$
$$= -A_i I_b Z_{out}. \quad (4)$$

We have put $I_2 = -A_i I_b$ in (4) and regard A_i as a positive number. The amplifier employed is a two-stage amplifier (standard grid input, plate output) so that output current has the same direction as the input current. A two-stage amplifier is employed since we want the input and output current to be in phase. Also

$$I_b = E_1/Z_b. \quad (5)$$

If we represent the parallel combined impedances R_1 and Z_b by Z_t, we have

$$\frac{1}{Z_t} = \frac{1}{R_1} + \frac{1}{Z_b} \quad (6)$$

and

$$E_1 = Z_t I_1. \quad (7)$$

One may re-draw the circuit as Fig. 4(c). From (4), (5) and (7),

$$E_2 = -Z A_i I_1 \quad (8)$$

where

$$Z = \frac{Z_{out} Z_t}{Z_{in}}. \quad (9)$$

Now writing loop equations involving currents I_1 and I_2 in Fig. 4(c), and equating the determinant of their coefficients to zero, one has

$$\begin{vmatrix} Z_t - (j/\omega C_1) & j/\omega C_1 \\ -(j/\omega C_1) - Z A_i & R_2 - (j/\omega C_1) - (j/\omega C_2) \end{vmatrix} = 0. \quad (10)$$

Since the real and imaginary part must vanish independently, we have

$$X_t(\omega) R_2 - \frac{1}{\omega^2}\left(\frac{1}{C_1} - \frac{1}{C_t(\omega)}\right)\left(\frac{1}{C_1} + \frac{1}{C_2}\right) + \frac{1}{\omega^2 C_1}\left(-\frac{1}{C_1} + \frac{A_i}{C(\omega)}\right) = 0 \quad (11)$$

$$\frac{X(\omega) A_i}{C_1} - X_t(\omega)\left(\frac{1}{C_1} + \frac{1}{C_2}\right) - R_2\left(\frac{1}{C_1} + \frac{1}{C_t(\omega)}\right) = 0 \quad (12)$$

where

$$Z_t = X_t(\omega) + \frac{1}{j\omega C_t(\omega)}, \qquad Z = X(\omega) + \frac{1}{j\omega C(\omega)}. \quad (13)$$

If the forms of functions $X_t(\omega)$, $C_t(\omega)$, $X(\omega)$ and $C(\omega)$ are determined, ω and A_i are obtained by solving (11) and (12) simultaneously.

In writing (13) we treat Z_t and Z as consisting of a resistive component plus a purely capacitive reactive component. This condition is sufficiently general for our purposes since our circuit contains no inductances.

Amplitude Stabilization

In order for the output of the oscillator to remain constant, it is necessary that E_2 increases when A_i decreases. Likewise when A_i increases E_2 must decrease.

To examine the condition for this requirement, consider the absolute value of (8) which may be written

$$|E_2| = A_i |Z|\,|I_1| \tag{14}$$

where

$$|Z| + \left[X^2(\omega) = \frac{1}{\omega^2 C^2(\omega)}\right]^{1/2}. \tag{15}$$

Then the stability condition may be written as

$$\frac{\partial |E_2|}{\partial A_i} < 0. \tag{16}$$

We now use the relation between ω and A_i such as (12), where

$$\omega = \omega(A_i).$$

Therefore (16) may be further calculated and gives

$$\frac{\partial |E_2|}{\partial A_i} = \left(\frac{\partial |Z|}{\partial \omega}\frac{\partial \omega}{\partial A_i} + |Z|\right)|I_1| < 0$$

or

$$\frac{\partial |Z|}{\partial \omega}\frac{\partial \omega}{\partial A_i} + |Z| < 0. \tag{17}$$

Solving (17) for A_i, one will obtain a range of values for A_i for which the amplitude of oscillation is stabilized. Such values of A_i will be less than a critical value which will be called α. Thus for allowable values of A_i one will have

$$A_i < \alpha.$$

On the other hand from (11), (12) one will obtain a minimum value of A_i (call it A_{ic}) below which oscillations will not occur. Thus permissible values of A_i will be bracketed by A_{ic} and α so that

$$A_{ic} < A_i < \alpha. \tag{19}$$

In designing the circuit then the parameters C_1, C_2, R_1 and R_2 must be selected so that (19) is satisfied.

In our case, we find that

$$\alpha = 2.28$$

$$A_{ic} = 1.97$$

when

$$C_1 = C_2 = 200 \times 10^{-12} F$$

$$R_1 = R_2 = 580 \times 10^3 \Omega$$

$$f = 1339 \text{ c/s}.$$

The required A_i is obtained by employing a 6SJ7 for voltage amplification and a 6K6GT tube for power amplification in a two-stage RC coupled amplifier.

Amplitude Control

The information contained in the formants is presented to the phototransistor as a change in the light intensity. Therefore the change of phototransistor characteristics with variation of light intensity must control the amplitude of the oscillator output. The method employed in the present application is to make use of the passive characteristics of a phototransistor.[5]

In Fig. 5 is shown a resistance-capacitance coupled, two-stage amplifier with typical values for the circuit elements. If a variable impedance Z is inserted between the two stages one may control the amplification factor for the circuit. For Z we employ a phototransistor and make use of the fact that its resistance will be a function of the incident light intensity.

Fig. 6 shows a schematic circuit with a phototransistor employed as a variable resistance element.

Fig. 7 shows collector voltage as a function of collector current when the transistor is exposed to light of fixed intensity.

As the light intensity is raised one will obtain a family of such characteristic curves. In the same figure is shown a "load line" that is a plot of the equation $V_B = I_c R_L + V_c$. Intersection of this line with the $V_c = V(I_c)$ curve determines the operating point.

If one now introduces a small ac voltage at the input ($v = v_0 \sin \omega t$) the new voltage and current across the phototransistor will be given by

$$V = V_c + v_0 \sin \omega t; \qquad I = I_c + i_0 \sin \omega t$$

thus

$$r = \frac{dV}{dI} = \frac{v_0}{i_0}.$$

This effective resistance to the ac component will be called the differential resistance.

For different light intensities, one will obtain a family of V-I curves. The differential resistance of the phototransistor for a given V-I curve is evaluated at the intersection of the dc load line and the V-I curve. In Fig. 8, the differential resistances obtained from such a family of illumination curves for a typical "load line" are plotted as a function of illumination. The voltage amplification constant for the circuit in Fig. 5 may be given as follows:

[5] Texas Instruments 800.

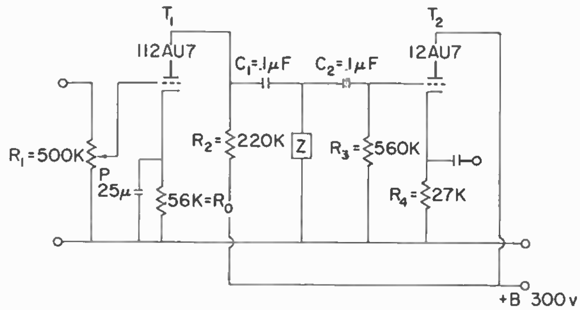

Fig. 5—Mixing circuit: Z represents phototransistor circuit.

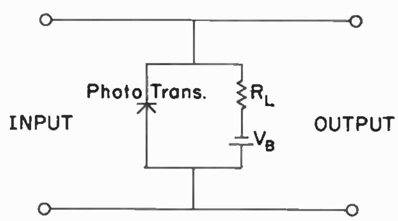

Fig. 6—Phototransistor circuit which is represented by Z in Fig. 5.

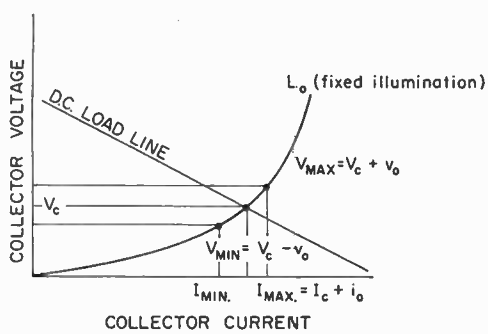

Fig. 7—Characteristic curve of diode and dc load line for a given illumination.

$$A = \frac{\mu_1\mu_2}{R_4 + r_{p_2}} \frac{R_4}{1 + r_{p_1}\left(\dfrac{1}{R_2} + \dfrac{1}{R_3} + \dfrac{1}{Z}\right)}$$

$$= \frac{\mu_1\mu_2}{R_4 + r_{p_2}} \frac{R_4}{1 + r_{p_1}\left(\dfrac{1}{R_2} + \dfrac{1}{R_3} + \dfrac{1}{R_L}\right) + \dfrac{r_{p_1}}{r}}$$

$1/Z = 1/R_L + 1/r$, since a resistance R_L is placed in parallel with the transistor.

μ_1, μ_2: Amplification constant for T_1 and T_2, respectively.

r_{p_1}, r_{p_2}: Plate resistance for T_1 and T_2, respectively.

Zi_r is obtained from Fig. 8 for a given illumination.

The amplification factor A as a function of illumination for the circuit of Fig. 4 is shown in Fig. 9. The ratio of the amplification factor at 200 foot candles to that at one foot candle is 100. This is a 40-db variation between on and off which is sufficient for our purposes. There is a slight residual sound when the circuit is in off condition. By introducing more circuit elements, it

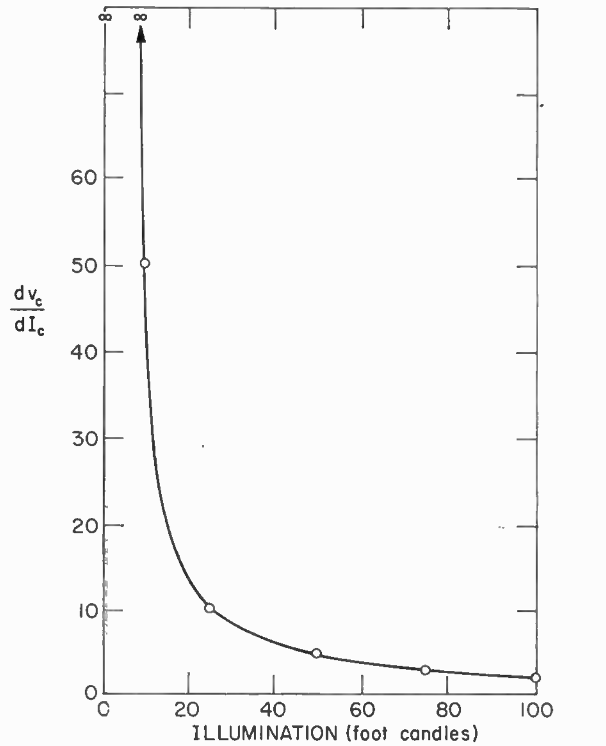

Fig. 8—The differential resistance vs illumination for phototransistor.

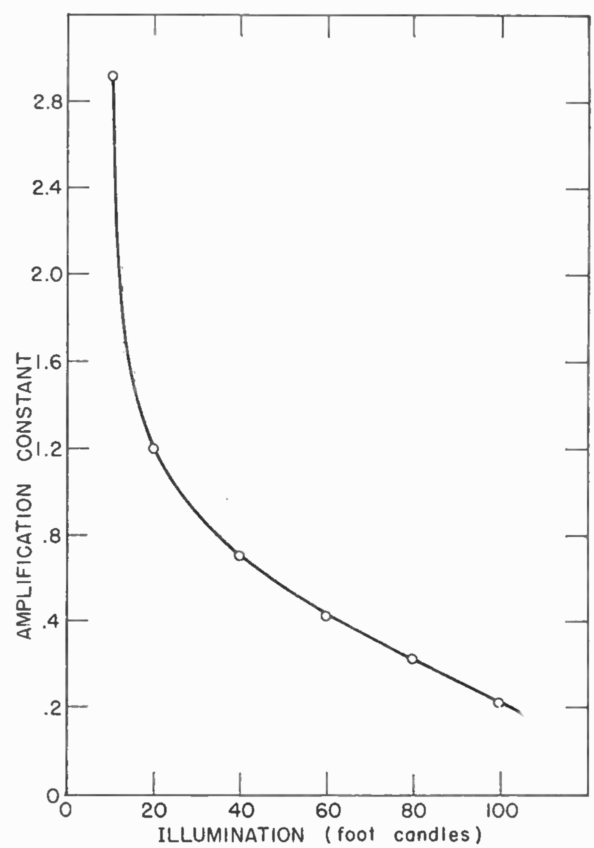

Fig. 9—Amplification factor A vs illumination for the circuit of Fig. 5.

would be possible to reduce the output voltage to zero when it drops below a critical minimum value. This has not been done in the present application.

A v_0 of 0.01 volt or less yields a sufficiently linear i_0. The 0.01-1-volt value for v_0 is obtained from a detailed study of the V-I characteristic curves and confirmed by experiment. The degree of amplitude modulation for each channel is monitored by means of a "magic eye."

A standard audio amplifier was employed in the output stage.

Conclusion

Speech synthesizing circuitry to be used with hand-painted spectrograms has been described. The prototype unit employing six oscillators was found to have excellent frequency stability for arbitrary settings of the oscillator frequencies. Photodiode control of the sound intensity produced the necessary flexibility for speech synthesis. With the introduction of additional oscillators one could obtain an instrument suitable for speech synthesis research purposes.

An Electron Cloud Head for Reproduction of Tape Recording*

MARVIN CAMRAS†, FELLOW, IEEE

Summary—**A compact flux sensitive head utilizes a diffuse electron stream which reverses direction in the region where the magnetic field is applied.**

IN PRINCIPLE any of the known electromagnetic effects may be used to play back the magnetic information on a tape recording. In practice most of the effects are of academic interest only, since they are small, or require elaborate equipment or adjustment. For this reason the simple coil-and-core combination utilizing electromagnetic induction has remained almost unchallenged.

The possibility of an electron beam transducer was suggested by A. M. Skellett in an early patent,[1] and later investigated by Skellett, Leveridge, and Gratian.[2] Skellett's transducer resembles a cathode-ray oscilloscope tube in which the beam deflection coils are replaced by polepieces that guide the magnetic flux from the tape. At the face end of the tube the beam strikes a pair of target plates. A signal from the tape deflects the electron beam, unbalancing the current to the target plates.

An advantage of this transducer is that its output is directly proportional to the flux picked up from the tape, rather than to rate-of-change of flux. Hence it can read a signal at very low speeds or even when the tape is not moving. The low-frequency response is inherently flat and does not require the usual 6 db per octave equalization.

On the other hand the beam tube is extremely sensitive to external magnetic fields including the earth's field. It requires a large shield, since the tube is rather bulky compared to a conventional head. Magnetic pole members must be included in the evacuated envelope. Also the electron beam may drift with changes in temperature or electrode voltages, so that readjustment is necessary.

Principle of Operation

The electronic head described in this paper operates in a somewhat different manner. As shown in Fig. 1, the envelope and base are made of parts from a standard miniature tube. The cathode is enclosed by element G_1 which has an opening in the front to allow passage of electrons. Element G_2 accelerates the electrons, which then pass through a larger opening in the center of a split electrode A_1–A_2. The result is a diffuse electron stream, or electron cloud directed into a narrow portion at the face of the tube. At the narrow section the electrons are decelerated, and finally reversed, since this region is near zero (cathode) potential. The reversed electrons are now attracted towards the split anode A_1–A_2, where they are finally picked up.

At the narrow portion in the tube face (which is actually formed from the sealing tubulation) U-shaped

* Reprinted from *J. Audio Engrg. Soc.*; October, 1963. Presented at the Audio Engineering Society Convention; October 21, 1962.

† Armour Research Foundation, Illinois Institute of Technology, Chicago, Ill.

[1] A. M. Skellett, "Means for translating magnetic variations into electric variations," U. S. Patent No. 2,165,307; July 11, 1939.

[2] A. M. Skellett, L. E. Leveridge, and J. W. Gratian, "Electron beam head for magnetic playback," *Electronics*, vol. 26, p. 168; October, 1953.

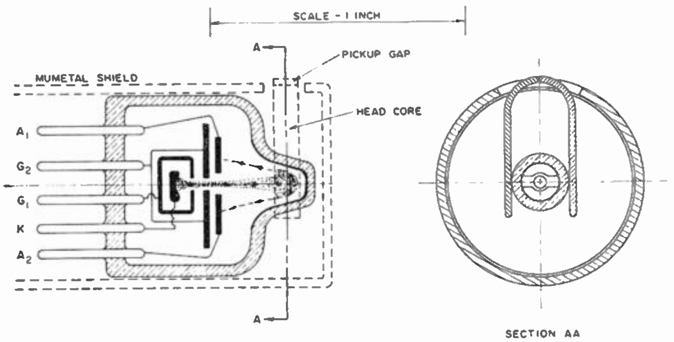

Fig. 1—Electron cloud head.

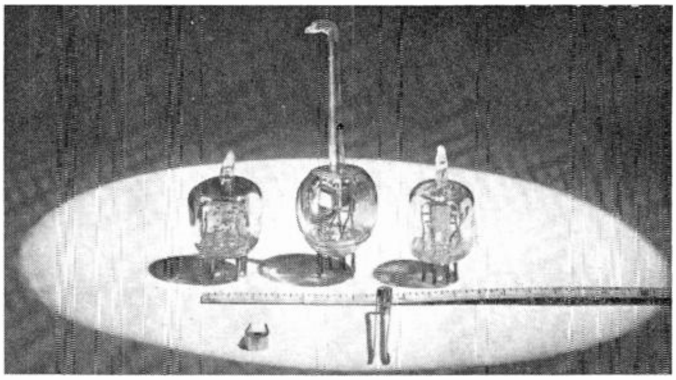

Fig. 2—Experimental electron cloud heads.

magnetic polepieces with a pickup gap are placed as shown in Fig. 1. These polepieces direct the magnetic field from the tape so that it acts on the reversing electrons, causing the return electrons to favor anode A_1 at the expense of A_2; or vice versa, depending on the instantaneous polarity of magnetization.

The constricted portion of the tube allows close magnetic coupling between the polepieces and the electrons in a region where the electrons are changing direction, and moving slowly. In this condition they are particularly sensitive to deflection by the field. To improve coupling, the tube wall may be flattened where it receives the polepieces, and the glass may be thinner in this area. With this design it is not necessary to seal any magnetic pole structure inside the tube envelope.

Experimental Results

Some experimental electron cloud tubes and associated polepieces are pictured in Fig. 2. The smaller versions are about an inch in maximum dimension, comparable in size to conventional pickup heads.

Circuit connections for the electronic head are shown in Fig. 3. The anodes are operated at a potential of only about 30 volts to give high deflection sensitivity. In the single ended circuit shown the output is taken from one anode, the other anode being held at fixed potential. The symmetrical anode structure is ideal for push-pull output if desired, but the single ended circuit is adequately low in distortion.

The output-vs-input curve in Fig. 3 shows that the linearity is excellent over a range of about 50 db before saturation takes place. Maximum output is approximately one volt across a one-megohm load resistor, using a test probe as a source of magnetic field at the gap of the pickup head.

Operating conditions are quite stable and noncritical. When the power line voltage is varied (with proportional changes of electrode potentials) the output remains practically constant until the voltage is reduced to below 100 volts. At 50 volts the sensitivity is reduced about 5 db (see Fig. 3). When the anode voltages are unbalanced by ratios of two to one, very little change is noticed in sensitivity.

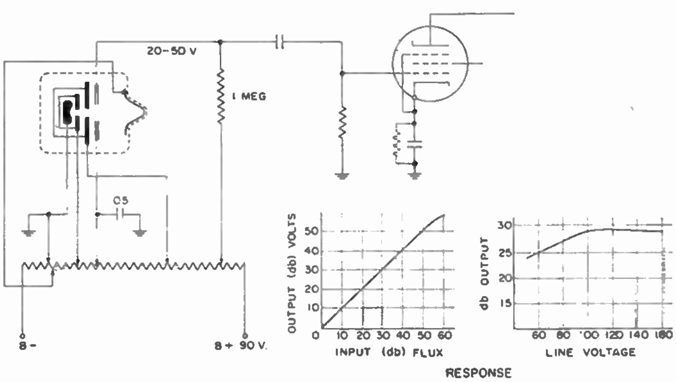

Fig. 3—Circuit for electron cloud head.

Comparison with Other Transducers

At one time electronic heads had the unique feature of sensing flux directly, but at present there are competitive types which also have this feature, the most successful being the magnetic modulator and the Hall-effect heads. It is interesting to compare these types.

Magnetic Modulator

The magnetic modulator head[3,4] is the most rugged and stable, being almost immune to electrical or mechanical damage, environmental effects or aging. Its output is high, in the order of a volt or more. There is nothing inherently expensive in its construction.

But the modulator head does require an oscillator (usually about 225 kc) to excite it, and its output must be demodulated. Upper frequency response is set by the oscillator frequency, by winding resonance and by core materials; however, the maximum limits have not been fully explored, so far. In earlier modulator heads a certain amount of Barkhausen noise was generated by the high-frequency excitation, and this was considered a limitation. Recent heads have a noise figure about 60 db below the signal, which brings it down to noise levels of the tape itself.

[3] D. E. Wiegand, "Electromagnetic head," U. S. Patent No. 2,855,464; October 7, 1958.

[4] M. E. Anderson, "New magnetic recording techniques for data processing," IRE Trans. on Industrial Electronics; vol. IE-10, pp. 47–52; December, 1959.

TABLE I
COMPARISON OF HEAD TYPES

Type of Head	Maximum Approx. Output Voltage 0.25-in Tape	Flux Sensitive	Impedance	Estimated Frequency Response	Ultimate Frequency Limitations	Reliability	Excitation Required	Noise	Can Use Also for Recording
Electronic	1.0	Yes	Very high	0–10 Mc	Electron transit time	Fair	Heater+ LV plate supply	Good	No
Magnetic Modulator	1.0	Yes	Low to high	0–10 Mc	Core materials Coil resonance	Excellent	HF Osc.	Good	Yes
Hall-Effect	0.0003	Yes	Low	0–>10 Mc	Circuit elements	Good	Direct current	Fair	No
Conventional (Rate-of-Change)	0.02	No	Low to high	20 cycles to >10 Mc	Low output at LF Coil resonance at HF	Excellent	None	Excellent	Yes

Hall-Effect

The Hall-effect head[5] uses a semiconductor element in place of a coil. It is simple to excite, requiring only a source of dc current. The sensing element is inherently flat from dc to the kilomegacycle range.

Some disadvantages arise from the fact that the Hall element is a thin film or wafer, comparable to a transistor in construction. It must be protected from mechanical fracture and electrical overloads. Sensitivity varies with temperature. Impedance is low and the output is only a fraction of a millivolt. If response to dc is needed, a better than average amplifier must be used. Hall elements generate a certain amount of noise which might be a problem in some applications; but usually this is masked by noise of the high gain amplifiers which must be used with these heads.

Electronic

The electronic head is a high-impedance device, giving higher output voltage than the Hall-effect type. Some interesting modifications are possible, as for example the incorporation of an electron multiplier to give higher sensitivity without the Johnson noise that occurs in amplifiers for all other types of heads. Another modification is to incorporate stages of amplification in the same tube envelope, so that the electronic head could operate a loudspeaker directly.

[5] M. Camras, "Some experiments with magnetic playback using Hall-effect sensitive elements," IRE TRANS. ON AUDIO, vol. AU-10, pp. 84–88; May–June, 1962.

Since there are no windings, the effects of coil resonance at high frequencies are avoided. Transit time may become a problem in the higher megacycle range. Power supply requirements for the electronic head are more complicated than for a Hall-effect head, but simpler than for a modulator head. The head described in Fig. 1 is stable, compact, and easy to shield.

An electronic head is subject to failure by burnout of the heater, or by damage to the glass envelope, and in these respects it is not as reliable as the modulator or Hall-effect heads. Of the three types, the electronic is probably the most expensive; although any of the heads can be produced at moderate cost if there is enough demand to allow quantity production.

Table I summarizes the above discussion, and also compares flux sensitive transducers with the more common rate-of-change heads.

CONCLUSIONS

An electron cloud head of improved stability and compactness has been described. Electronic heads have advantages in output and in circuitry compared to other kinds of flux sensitive transducers.

Modifications are possible which avoid input stage "Johnson noise," or which eliminate the need for additional amplifiers.

Correction

Donald F. Eldridge, author of "A Special Application of Information Theory to Recording Systems," which appeared in the January-February, 1963 issue of these TRANSACTIONS, has requested that a statement be published that this paper was based upon work which he performed while employed by the Research Division of Ampex Corporation.

Unified Analysis of Tracing and Tracking Error*

DUANE H. COOPER†

Summary—Tracing and tracking errors in phonograph reproduction are shown to have a common basis of analysis, the skew transformation, and the distortion arising from these errors to be due solely to phase perturbation. The phase-perturbation model is used to show the principles by which compensating schemes must be governed. Formulas are given for the distortion arising from the joint application of tracing and tracking error, and the recording-velocity restrictions so implied are plotted. In the Appendix, a means for obtaining exact closed-form Fourier analyses is explained and results quoted.

Introduction

NUMERICAL ANALYSIS[1,2] and development in power series[3,4] have been the two most successful schemes for the calculation of the distortion resulting from tracing error in phonograph reproduction. It seems not to have been noticed that tracing error may be represented entirely by a phase perturbation, and that useful results may be calculated, as has been done recently for tracking error,[5] basing the analysis on that perturbation. The gist of the matter is that the tracing transformation, by which tracing error is generated, when put into the form for application to the slope waveform, is seen to be nothing but a normalized skew transformation, or a generalization of it. Since tracking distortion is also generated by the skew transformation applied to the amplitude waveform,[6] it follows that these two errors have a common basis for analysis.

Here, after showing the role of the skew transformation in generating tracing error, a few abstract properties of that transformation are developed. Then an operational model, as for an electronic analog computer, is given, representing the skew transformation in its phase-perturbing character. It is shown how such a model could be applied, in principle, to electronic compensation for tracing and tracking error.

The method of phase perturbation is then used to derive formulas for the harmonic distortion and intermodulation distortion, resulting from simultaneous tracing and tracking error, when the distortion is small. Numerical examples are presented, showing how these formulas could be used to derived bounds on the recording velocities, in making stereo discs, if both harmonic and intermodulation distortion are to be bounded, in the absence of any compensation.

Finally, in the Appendix, it is shown how an exact Fourier analysis may be given, in closed form, for the distorted waveform resulting from the application of the skew transformation to sinusoidal waveforms or finite linear combinations of them. Explicit results are presented for the single-tone case, as well as for the two-tone case used in intermodulation testing.

Analysis of Tracing Error

The notation, shown in Fig. 1, is adapted from Lewis and Hunt.[3] The shape of the tracing stylus is described in local (δ, σ) coordinates by the function

$$\sigma = c\Phi(\delta/c), \tag{1}$$

assumed to be monotonically curving, convex downwards, and with vertex at the origin of the local coordinates. The parameter c is used to designate the vertex radius of curvature. The stylus is assumed to make a single-point contact with the curve

$$\eta = \eta(\xi), \tag{2}$$

described in the fixed coordinate system, with η playing the role of y, and ξ that of x. The contact is at the point ξ, η. The origin of the local coordinates is designated by x, y, and, as the stylus slides along, it traces the curve

$$y = y(x), \tag{3}$$

which is a distorted version of the given $\eta(\xi)$ curve.

Tangency at the point of contact requires the matching of slopes:

$$\Phi'(\delta/c) = \eta'(\xi). \tag{4}$$

Also, the slope at the corresponding point on $y(x)$ is the same:

$$y'(x) = \eta'(\xi), \tag{5}$$

where the prime denotes differentiation. Eq. (4) may be solved for $\delta = \xi - x$, and the solution represented by the inverse function g, taken to be the inverse of Φ':

$$\delta = \xi - x = cg(\eta'). \tag{6}$$

Thus, the transformation from ξ, η to x, y is represented by

$$\begin{aligned} \xi &= x + cg(y'), \\ \eta' &= y', \end{aligned} \tag{7}$$

* Manuscript received July 19, 1963. This work was done, in part, as Consultant to Consumers Union, Mount Vernon, N. Y.

† Coordinated Science Laboratory and Department of Electrical Engineering, University of Illinois, Urbana, Ill.

[1] J. A. Pierce and F. V. Hunt, "On distortion in sound reproduction from phonograph records," *J. Acoust. Soc. Am.*, vol. 10, pp. 14–28; July, 1938.

[2] M. S. Corrington and T. Murakami, "Tracing distortion in stereophonic disc recording," *RCA Rev.*, vol. 19, pp. 216–231; June, 1958.

[3] W. D. Lewis and F. V. Hunt, "A theory of tracing distortion in sound reproduction from phonograph records," *J. Acoust. Soc. Am.*, vol. 12, pp. 348–365; January, 1941.

[4] M. S. Corrington, "Tracing distortion in phonograph records," *RCA Rev.*, vol. 10, pp. 241–253; June, 1949.

[5] D. H. Cooper, "Tracking distortion as phase modulation," IEEE Trans. on Audio, vol. AU-11, pp. 41–46; March-April, 1963.

[6] H. G. Baerwald, "Analytic treatment of tracking error and notes on optimal pick-up design," *J. SMPE*, vol. 37, pp. 591–622; December, 1941.

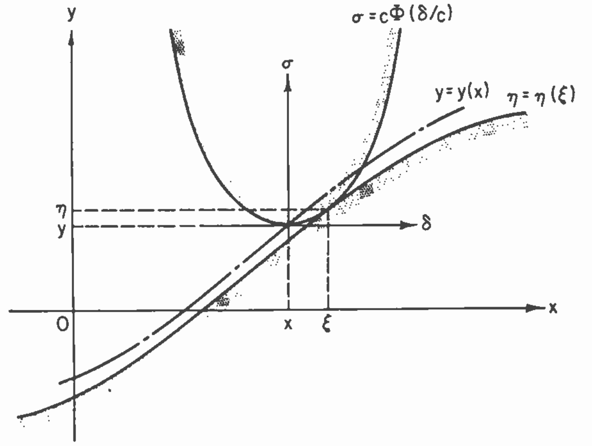

Fig. 1—Tracing error notation. The curve $\sigma = c\Phi(\delta/c)$ describes the tracing-stylus shape in the local δ, σ coordinates, whose origin is the point x, y. The stylus slides on the curve $\eta=\eta(\xi)$ to trace the curve $y=y(x)$. The x, y coordinates of the point of contact are ξ, η. The parameter c is the vertex radius of curvature of the stylus.

which is seen to actually connect the pair ξ, η' with the pair x, y'.

In the case for which the stylus has a parabolic tip:

$$\sigma = \delta^2/2c, \tag{8}$$

the tracing transformation, T_c, becomes simply

$$\begin{aligned} \xi &= x + cy', \\ \eta' &= y', \end{aligned} \tag{9}$$

which is the form of the normalized skew transformation, discussed below.

In more general cases, it is customary to restrict consideration to symmetrical styli. Then, if Φ is even, g is odd, and, under these circumstances, (7) is a reasonable generalization of the normalized skew transformation for slopes. Odd Φ have no interpretation for tracing waveforms, for then there could not be a simple tangent point of contact, although Φ could have an odd part, so long as the even part were dominant. One of the more commonly cited cases is that of the conical stylus whose tip is rounded to the form of a spherical cap. In that case the function g is

$$g = y'[1 + (y')^2]^{-1/2}. \tag{10}$$

This form of g is not used in the present paper for several reasons. One is that it invokes complications of no theoretical interest. A second is that it presumes an unwarranted precision in the knowledge of the shape of the stylus tip, in comparison with simpler assumptions, such as that of the parabolic tip, given preference here. A third reason is that the spherical assumption gives different results from the parabolic only for large distortions, and it is felt that cases of large distortion are not only uninteresting, but not susceptible to precise calculation, on kinematic grounds alone.[7] An exception is the case of purely lateral (monaural) recording. For the purely lateral mode, the even-order tracing distortion cancels, so that the third-order distortion becomes the dominant one. While the present work confines its attention to the stereo case, it may be adapted to the lateral case, but then the arguments for rejecting (10) would be somewhat weakened. One may still doubt whether a purely kinematic treatment is adequate for the lateral case, however, even for the calculation of moderate amounts of distortion.

[7] J. Walton, "Stylus mass and reproduction distortion," *J. Audio Engrg. Soc.*, vol. 11, pp. 104–109; April, 1963.

The Normalized Skew Transformation

The skew transformation connects one set of skew coordinates ξ, η, with skew angle ψ, to another set x, y where the x axis is parallel to the ξ axis, but the y axis is tipped away from the normal by the angle $\psi+\phi$. The equations are

$$\begin{aligned} \xi &= x + y \sin\phi/\cos\psi, \\ \eta &= y\cos(\psi+\phi)/\cos\psi. \end{aligned} \tag{11}$$

If y or η is always to be a dependent variable, then there is usually little interest in a constant dilatation along that axis, so that one introduces a parameter of skewness

$$k = \sin\phi/\cos(\psi+\phi),$$

and speaks of the normalized skew transformation, T_k:

$$\begin{aligned} \xi &= x + ky, \\ \eta &= y. \end{aligned} \tag{12}$$

These equations described the effect of a tracking angle error ϕ, in phonograph reproduction, analogous to the tracing error in the manner described above.

The normalized skew transformation carries the function $\eta=f(\xi)$ into the function

$$y = f(x + ky), \tag{13}$$

which may be interpreted recursively to be

$$y = f(x + kf(x + \cdots)), \tag{14}$$

a form which could be called a continued function by analogy with "continued fraction." In (13) or (14), the phase perturbing character of the transformation is evident.

The skew transformation obeys the functional equation for the exponential:

$$T_kT_j = T_{k+j}. \tag{15}$$

This is shown by writing for T_j

$$\begin{aligned} x &= \bar{x} + j\bar{y}, \\ y &= \bar{y}, \end{aligned}$$

for application to (13), with the result

$$\bar{y} = f(\bar{x} + j\bar{y} + k\bar{y}) = f(\bar{x} + (k+j)\bar{y}),$$

which may be interpreted in the same manner as in (14).

Also from (15) it is seen that inverse of T_k is

$$T_k^{-1} = T_{-k}, \tag{16}$$

since the product with T_k is the identity transformation, I.

A related transformation is R_y, that of reflection

$$\begin{aligned}\bar{\xi} &= \xi,\\ \bar{\eta} &= -\eta.\end{aligned} \tag{17}$$

It carries $\bar{\eta}=f(\bar{\xi})$ into

$$\eta = -f(\xi).$$

Thus, T_kR_y carries f into

$$y = -f(x+ky) = -f(x-kf(x-\cdots)),$$

so that the application of $R_yT_kR_y$ to f results in

$$y = f(x-ky) = f(x-kf(x-\cdots)),$$

which is just the result of applying T_{-k}. The conclusion is that

$$T_k^{-1} = T_{-k} = R_yT_kR_y. \tag{18}$$

All of these abstract properties, regarding (15), (16) and (18), are shared with T_θ, the rigid body rotations about a single axis.[8] This is not surprising, in view of the representation (12), which may be regarded as defective rotation equations. The generalization of the normalized skew transformation, as in (7), also shares these properties so long as g is odd.

Operational Representation

The phase perturbations which are the cause of both tracing and tracking distortions may be visualized in terms of the operations performed by elements of an electronic analog computer. Apart from being helpful in visualization, these operational models could be the basis for devising means for compensation to remove such distortions. Although the models to be developed are unquestionably realizable in principle, there could be difficulties in practice, because of the need for a signal-controllable delay.

Fig. 2 shows the operations involved in generating tracking distortion. If the input is to be $f(t+t_0)$, where t_0 is the delay to the mid-point of the delay line, considered to be the zero for the sliding tap, then the output is $f(t-kf(t-\cdots))$. The sign of k is here chosen to correspond to inclinations of the plane of the stylus motion, forward in the direction of the groove motion, a clockwise tipping viewed from the turntable spindle, so that upward motions do delay the response. The amplifiers shown are intended to be noninverting. If both are of the inverting type, the effect is the same as reversing the polarity of the mechanism that causes the sliding tap to move, as shown above in (18). The tap-moving mechanism causes motion varying as kf, and it is called *k-delay actuator* in the figure. The representation is for the amplitude mode. For the velocity mode, the input amplifier would also have to undo the velocities, *i.e.*, integrate, followed by conversion back to the velocity mode by differentiation in the output amplifier.

Fig. 3 shows the operations involved in generating tracing distortion. Again, the representation is for the amplitude mode, so that the necessary conversion is built into the amplifiers. The block called *Non-linear* is to have an odd-transfer function not involving any memory, since all energy-storage devices needed, except for mode conversion, reside in the delay line. In representing the effect of a parabolic tip, that block becomes linear and merely passes the velocity signal along to the *c-delay actuator*, in close analogy with Fig. 2.

The ease with which inverses to these transformations may be realized, conceptually, facilitates the consideration of general principles to which any compensating mechanism must conform. For example, phase automodulation and a linear operation, such as integration or differentiation, do not commute, so that T_c and T_k will not commute, nor will their inverses. For this reason, attention must be paid to the order in which these processes are to be invoked. In playback, tracing error comes before tracking error, and it follows that the compensation to come after playback would have to present the inverses in reversed order, as in Fig. 4. However, it is not possible, in view of Walton's results,[7] to remove large amounts of distortion in this way. Such large amounts may only be prevented by pre-compensation as in Fig. 5.

Fig. 5, however, is based on the use of a cutting action that is truly normal to the groove axis. If the effective cutting action is at some other angle, exact compensation is more complicated. Then, the cutter is already providing compensation for some skewness parameter $\bar{k}$, in effect. The trouble is that tracing compensation is the one that is to just precede cutting. Thus the tracking compensation "built-in" the cutter has to be undone so that tracing compensation can come in the correct sequence. The full sequence of transformations is shown in Fig. 6.

The distortion caused by polishing facets on the cutting stylus may be represented by a tracing transformation and treated in a similar manner. Always, of course, the success of tracing compensation is bounded by a maximum-curvature limitation, analogous to a maximum-slope limitation for tracking-distortion compensation. Also the cutting bandwidth has to be sufficient, for pre-compensation, to pass all harmonics generated by the inverse transformations. Hunt argues that this implies a doubling of the usual bandwidth.[9]

Hunt also points out[9] that a mechanical inverse to T_c has been known since 1938. It has been attributed[3] to

[8] H. Margenau and G. M. Murphy, "The Mathematics of Physics and Chemistry," D. van Nostrand Co., Inc., New York, N. Y., pp. 550–554; 1943.

[9] F. V. Hunt, "The rational design of phonograph pickups," *J. Audio Engrg. Soc.*, vol. 10, pp. 274–288; October, 1962.

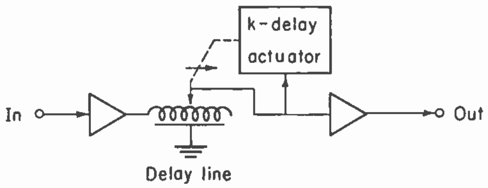

Fig. 2—Operational model of tracking transformation, T_k. The *k-delay actuator* causes the delay-line tap to move in proportion to the signal in the output, positive signals causing positive delay increments. The amplifiers are non-inverting, unless the inverse transformation is to be represented.

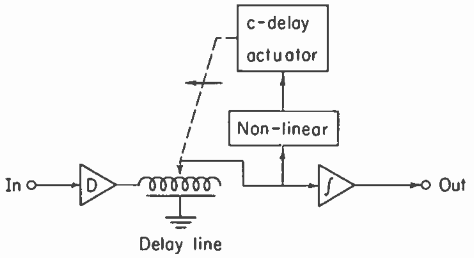

Fig. 3—Operational model of tracing transformation, T_c. The *c-delay actuator* causes the delay-line tap to move in proportion to the velocity of the signal in the output, or that velocity subject to an odd nonlinear, but memory-less, transformation. Positive velocities cause delay decrements. The amplifiers are as in Fig. 2 except for the operations of differentiation and integration, with respect to time, indicated.

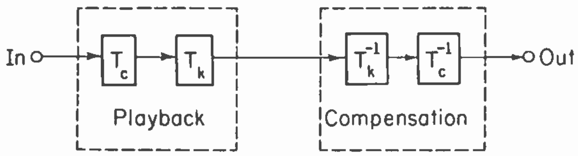

Fig. 4—Playback compensation. The diagram shows the order in which the inverses of the operational transformations would have to be applied.

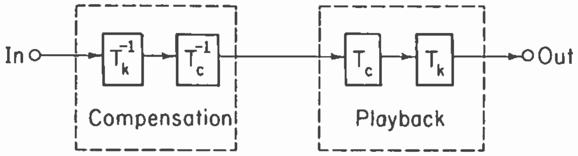

Fig. 5—Pre-playback compensation. The diagram shows the order in which the inverses of the operational transformations would have to be applied, prior to playback, or if only an ideal cutter intervened.

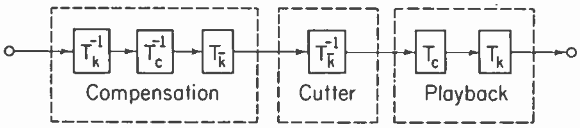

Fig. 6—Pre-playback compensation for a tipped cutter. The cutter is supposed to provide for a skewness $\bar{k}$, but to be otherwise ideal.

MacNair. By means of re-recording upon playback, but with reversed polarity, one can generate

$$T_c^{-1} = R_y T_c R_y,$$

a trick which will also work for tracking distortion, as has been shown here. The applicability of mechanical compensation to tracing and tracking error jointly has also been discussed.[10]

Distortion Calculations

The present calculations are to take into account only the kinematic effects of tracking and tracing error. For this reason, as has been stated before, the calculations must be confined to the case when the distortions are small, for only then do these distortions dominate all others. Under these circumstances, the phase perturbation method, as worked out elsewhere,[5] is appropriate. Methods for exact calculations in closed form may be found in the Appendix.

Here, it suffices to list the various modulation indices without repeating their derivations, for which appeal is made to the earlier work just cited. The phase automodulation indexes are

$$\begin{aligned} \beta_{k1} &= (2\pi A_1/\lambda_1)k \approx (v_1/v_g)\phi, \\ \beta_{c1} &= (2\pi/\lambda_1)(v_1/v_g)c = (2\pi\nu_1/v_g)(v_1/v_g)c, \end{aligned} \tag{19}$$

for tracking and tracing distortion, respectively. In the amplitude mode, the second harmonic content is $\beta_{k1}/2$ and $\beta_{c1}/4$. The extra factor 1/2 appears for tracing distortion, upon converting to the amplitude mode, because of the reduced sensitivity to the second harmonic that such a mode conversion entails. Here, the amplitude is A_1; the wavelength is λ_1; the recording velocity is v_1; the groove speed is v_g; and the frequency is ν_1. The parameter of skewness is written simply as ϕ, in radians, as an adequate approximation to $\sin\phi/\cos(\psi+\phi)$, for most cases of interest. The formula for β_{c1} is simply the ratio of the peak curvature of the waveform to the curvature of the stylus, a useful mnemonic.

The phase intermodulation indexes are

$$\begin{aligned} \beta_{k2} &= (\nu_2/\nu_1)(v_1/v_g)\phi, \\ \beta_{c2} &= (\nu_2/\nu_1)(2\pi\nu_1/v_g)(v_1/v_g)c, \end{aligned} \tag{20}$$

and are direct measures of the phase intermodulation distortion. The amplitude intermodulation distortion is not taken into account in these calculations, because it is so much smaller than the phase intermodulation, and the ear is not less sensitive to the latter.[5]

It is possible to combine the distortion measures from tracing and tracking error. The skew transformation preserves the antisymmetry of an f assumed antisymmetric, as may be seen from (14). Thus, if the slope waveform had been a sine series, the result of tracing distortion is again a sine series, which becomes, in the amplitude mode, a cosine series. However, the applica-

[10] D. H. Cooper, "Compensation for tracing and tracking error," *J. Audio Engrg. Soc.*, vol. 11, pp. 318–322; October, 1963.

tion of cosine phase modulation in a cosinusoidal function yields odd-order terms which are sines. Since it is the odd-order terms which are used to measure the harmonic and phase intermodulation distortion, when the distortion is small, it is observed that the tracking-distortion terms are in phase quadrature with the tracing-distortion terms. Thus, the distortion indices combine by the root-sum-of-squares rule. The total harmonic distortion is

$$D_{\mathrm{THD}} = 100[(\beta_{k1}/2)^2 + (\beta_{c1}/4)^2]^{1/2} \qquad (21)$$

per cent, and the total phase intermodulation distortion is

$$D_{\mathrm{TPIM}} = 100[\beta_{k2}{}^2 + \beta_{c2}{}^2]^{1/2} \qquad (22)$$

per cent.

If bounds are to be placed on these distortion figures, it is possible to calculate the bounds thereby imposed on recording velocity. Inserting the values for the modulation indexes from (19) and (20) into (21) and (22) and solving for v/v_g, one obtains

$$(v_1/v_g) = (D_{\mathrm{THD}}/50)[(\pi\nu_1 c/v_g)^2 + \phi^2]^{-1/2}, \qquad (23)$$

$$(v_1/v_g) = (D_{\mathrm{TPIM}}/200)(\nu_1/\nu_2)[(\pi\nu_1 c/v_g)^2 + (\phi/2)^2]^{-1/2}, \qquad (24)$$

upon which numerical calculations are easily based.

Numerical Examples

For making numerical calculations from (23) and (24), definite choices of distortion figures must be made. For purposes of illustration, the choices may be arbitrary, yet if the results are to be physically meaningful the distortion figures may not be large. Fortunately, if one is seriously considering high-fidelity standards, there is also little interest in large distortion figures. The numbers here chosen are 2 per cent THD and 10 per cent TPIM.

These numbers will seem large to amplifier engineers as high-fidelity-rating standards. It should be remembered, however, that only a small sacrifice in the power rating of an amplifier can accommodate a large reduction in distortion rating, so catastrophically does the distortion increase, in most vacuum-tube-feedback amplifiers, once it begins. Thus, for amplifiers, the distortion-limited-power rating has its most meaningful reference to absolute peaks in level. Here, the distortion is proportional to level, so that an attempt to assess the permissible level with respect to some kind of VU-reference makes more sense. The thought is that distortion causes less annoyance, if it is not catastrophic, and if it is of lesser duration, than otherwise, so that the integration of short term peaks, provided by a VU-meter, is appropriate. A consequence is that, if the above figures are taken as setting a VU maximum, then levels giving roughly three times as much distortion will occur, unnoticed on the VU-meter, and hopefully unnoticed by the ear. In any case, the numerical results may be readily reinterpreted for smaller distortion figures.

In passing, it may be mentioned that, if full compensation for tracing and tracking error were in use, an absolute peak-level-rating scheme would be appropriate, since, once the compensation reached its theoretical limits, and began to fail, it could fail catastrophically.

Choices also have to be made of the stylus-tip radius and tracking-angle error. For the former, high-fidelity standards suggest 0.5 mil, as a low figure currently within the state of the art. For the latter, the resulting plots are not too confusing if a spectrum of angles is selected. These are 2, 4, 8, 16, and 32 degrees. The spacing of the contours allows one to assess, also, which of the two, tracing or tracking error, is the more severe limitation at any one frequency.

Finally a choice of the upper frequency, for the intermodulation calculation, must be made. Five kilocycles was chosen, again somewhat arbitrarily, but with the thought that higher frequencies actually carry less information, serving only to add a certain sonic sheen, and could tolerably suffer somewhat greater intermodulation than the quoted 10 per cent. Of course, all of these choices should be made only after the most careful psychoacoustic studies had been made. The author has sought only to make "reasonable" choices, so that explicit numerical examples might be given.

The numerical results are given in graphs. In Fig. 7, recording velocity, considering only the 2 per cent limitation in total harmonic distortion, is plotted vs frequency for the various tracking angle errors, and the standard tracing error resulting from the half-mil stylus. The vertical scale on the left is the peak recording velocity in decibels, the reference being the groove speed, here taken to be 10 inches per second. The vertical scale on the right is the rms velocity in decibels, the reference being the rms velocity of 1 centimeter per second. It is easy to see which parts of the contours are governed by tracking error and which by tracing error.

Part of the peculiarities in shape is a reflection of the enhanced sensitivity to the second harmonic that the RIAA equalization curve produces. Parts of that curve show a slope not quite so steep as the negative 6-db-per-octave-velocity correction. Or, to put it another way, the RIAA equalization produces a nearly constant-amplitude sensitivity, except for regions of positive slope. In the lower treble, for example, there is a region of positive slope, enhancing sensitivity to the second harmonic by some 3.6 db, at 750 cps. Another such region occurs in the bass. In Fig. 7, the curve marked RIAA shows the enhanced sensitivity. The dashed line, drawn with negative slope, shows the velocities at which any scheme of tracing compensation would fail, since, along that contour, the peak curvature of the recorded wave would match that of the stylus.[11]

[11] *Note added in proof:* The curvature limits shown in Figs. 7 and 9–11 have been unaccountably misplotted. They should be displaced to the right one full octave.

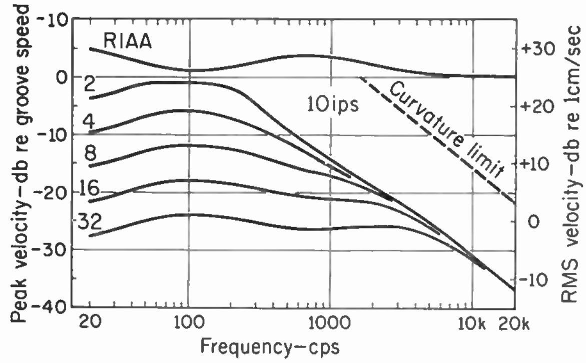

Fig. 7—Recording velocities limited by 2 per cent harmonic distortion. The distortion is the quadrature sum of tracing and tracking distortion, for the tracking angle errors of 2, 4, 8, 16, and 32 degrees, and for a tracing stylus of a half-mil radius. The sensitivity to the second harmonic, characteristic of the RIAA curve, is shown, and its influences on the constant-distortion contours may be seen. The groove velocity is 10 inches per second.

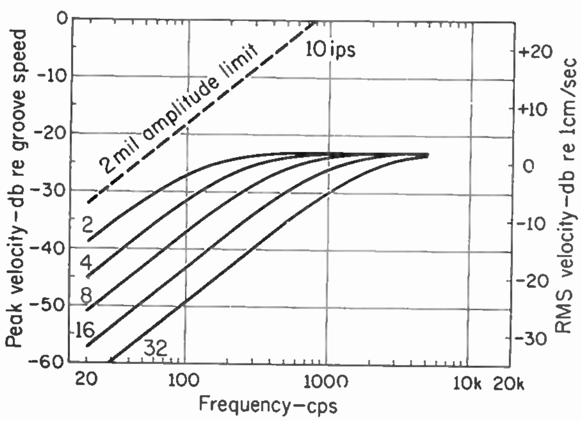

Fig. 8—Recording velocities limited by 10 per cent intermodulation distortion. Phase intermodulation of a 5-kc carrier, by lower frequency tones, resulting from the joint effects of tracing and tracking error, and not to exceed 10 per cent PIM, sets the velocity contours. Otherwise, the conditions are as for Fig. 7.

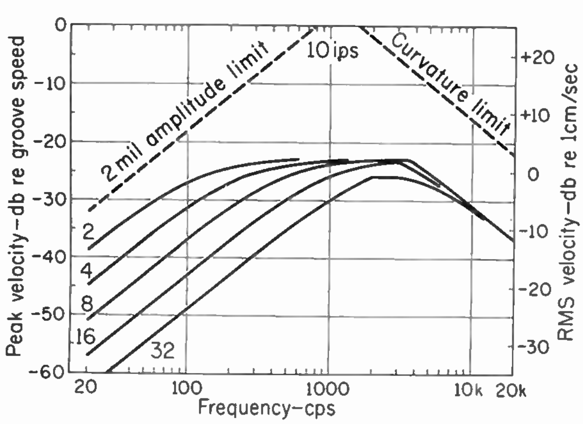

Fig. 9—Recording velocities limited by 2 per cent THD or 10 per cent TPIM. The contours combine the data from Figs. 7 and 8. Phase intermodulation controls the velocity at low frequencies, and harmonic distortion does so at the higher frequencies. Again, the groove speed is 10 inches per second.

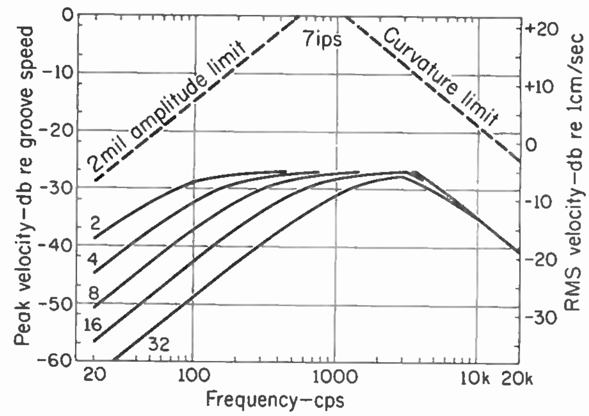

Fig. 10—Recording velocity limitations at 7 inches per second. The same conditions as for Fig. 9, except for the 7-inch-per-second-groove speed, obtain.

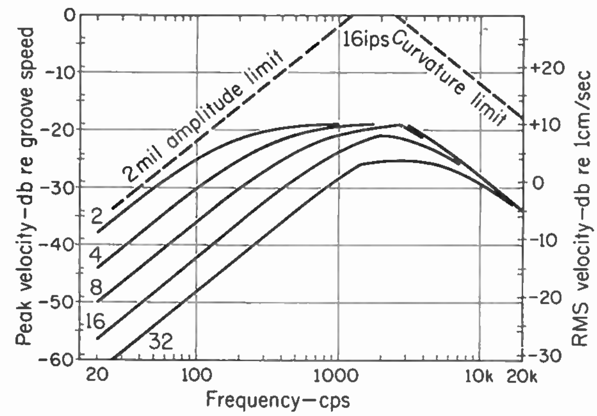

Fig. 11—Recording velocity limitations at 16 inches per second. The same conditions as for Fig. 9, except for the 16-inch-per-second-groove speed, obtain.

The curves in Fig. 8 are for a total phase intermodulation distortion of 10 per cent. Again it is easy to tell which parts are governed by tracking error and which by tracing error. The various scales have the same meaning as before. The groove speed is again 10 inches per second. The positively sloping dashed line is for an arbitrarily chosen 2-mil amplitude limit.

In Fig. 9, the results of Fig. 7 and Fig. 8 are combined. Total phase intermodulation, at 10 per cent, governs the lower frequencies, and total harmonic distortion, at 2 per cent, governs the higher frequencies. The transition between the two regimes may be clearly seen. Figs. 10 and 11 are like Fig. 9, but are plotted for groove speeds of 7 and 16 inches per second, respectively.

From these charts, the conclusion that tracing and tracking distortion can impose severe limitations on recording velocity is inescapable. Surprisingly enough, a rough survey suggests that a fair number of stereo recordings have been produced, in the past five years, that obey these limitations, in a VU sense, if not in an absolute peak-level sense, and if one measures only vertical modulation. Not so surprisingly, those recordings sound quite decent. Again, it is not surprising that records which systematically and severely violate such limitations sound bad, and that their number appears to be legion.

It is disappointing that, while large tracking errors impose especially severe limitations on recording velocity, the reduction of these errors to near 2 degrees still leaves a severe limitation, imposed largely by tracing error. There is hope, however, that the development of compensation would allow velocities approaching the dashed contours to be recorded, at least in an absolute peak-level sense, and with every expectation of low distortion.

Appendix

Exact Analysis

A defect of the method of phase perturbation is that in first order it requires the truncation of

$$y(x) = f(x + kf(x + \cdots)) \tag{25}$$

to

$$y(x) \approx f(x + kf(x)), \tag{26}$$

so that the results are not in closed form, and require kf to be small. The peak phase-modulation indexes are, however, exact, since the normalized skew transformation does not change the values at extrema; the inexactness results from not taking the skewness of the modulation itself into account. Carrying the calculation to higher order in phase perturbation can be excessively laborious, because of the multiple convolutions involved. Also, only theoretical interest attaches to the slightly more precise result. Another way to satisfy that interest is explained here.

It is always possible, in principle, to insert a function given only parametrically into the Fourier analysis integral

$$\int ye^{-i\omega x}dx, \tag{27}$$

so that, if the parameter be called s, one is confronted with the evaluation of

$$\int y(s)x'(s)e^{-i\omega x(s)}ds. \tag{28}$$

When the skew transformation, solved for x and y,

$$\begin{aligned} x &= \xi - k\eta(\xi), \\ y &= \eta(\xi), \end{aligned} \tag{29}$$

is inserted into (28), however, one has

$$\int \eta(\xi)[1 - k\eta'(\xi)]e^{ik\omega\eta(\xi)}e^{-i\omega\xi}d\xi, \tag{30}$$

which is tractable for sinusoidal, or finite linear combinations of sinusoidal, functions for $\eta(\xi)$. In the case of the linear combinations, one still has the labor of multiple convolutions, but these are of finite order and have the rewarding property of giving exact results.

The integral (30) resembles the analysis of

$$h(\omega, \xi) = \eta(\xi)[1 - k\eta'(\xi)]e^{ik\omega\eta(\xi)}. \tag{31}$$

This resemblance can be deceptive, because (31) has the analysis variable ω as a factor in its exponent. A convenient way to evaluate (30) has been found to be the Fourier analysis of (31) in terms of some new frequency variable Ω, treating ω as a free parameter. For this, general methods may be used, or equivalent special methods, such as trigonometric identities, convolution, modulation theory, rotating vectors, etc., may be helpful. In particular, the Fourier series due to Jacobi

$$e^{i\beta \sin \omega_1\xi} = \Sigma_n J_n(\beta)e^{in\omega_1\xi}, \tag{32}$$

in which the summation ranges over $-\infty < n < \infty$, and $J_n(\beta)$ is the Bessel coefficient of the first kind, order n, is needed.[12]

Proceeding in this way, one obtains the Fourier series representation of (31),

$$h(\omega, \xi) = \Sigma_n H(\omega, \Omega_n)e^{i\Omega_n\xi}, \tag{33}$$

in standard form. It is often helpful to study the properties of (33) for certain critical values of ω, often at $\omega = 0$, for example, but (33) represents only an intermediate result. It is to be inserted into (30), whose evaluation is now trivial. One obtains, finally

$$y(x) = \Sigma_n H(\omega_n, \omega_n)e^{i\omega_n x}, \tag{34}$$

and has achieved the elimination of the parameter, ξ. For the particular choices of the function $\eta(\xi)$, assumed, the Fourier coefficients H will be finite combinations of Bessel coefficients and, hence, of closed form.

This program of analysis has been carried through for the single-tone case and for the two-tone case, as for intermodulation testing. For the single-tone case, the result is[6]

$$y(x) = A\Sigma_n(2/n\beta_1)J_n(n\beta_1) \sin n\omega_1 x, \tag{35}$$

stemming from

$$n(\xi) = A \sin \omega_1\xi,$$

and in which β_1 is $kA\omega_1$, and the summation ranges over $1 \leq n < \infty$.

Moderately extensive manipulations are involved in obtaining the result (35) including liberal application of the recurrence relation,[11]

$$(2n/u)J_n(u) = J_{n-1}(u) + J_{n+1}(u), \tag{36}$$

[12] E. T. Copson, "Theory of Functions of a Complex Variable," Oxford University Press, London, England, p. 321; 1935.

and symmetry properties,

$$J_n(-u) = (-1)^n J_n(u),$$
$$J_{-n}(u) = (-1)^n J_n(u), \tag{37}$$

but even more extensive manipulations, also invoking these, are required to obtain the two-tone result,

$$y(x) = A\Sigma_{m,n} H_{m,n} \sin \omega_{m,n} x, \tag{38}$$

in which the notations

$$H_{m,n} = 2J_m(\epsilon\beta_{m,n})J_n(\beta_{m,n})/\beta_{m,n},$$

and

$$\omega_{m,n} = m\omega_2 + n\omega_1,$$
$$\beta_{m,n} = m\beta_2 + n\beta_1 = kA\omega_{m,n}$$

are used. All this stems from writing for $\eta(\xi)$ just

$$\eta(\xi) = A(\sin \omega_1\xi + \epsilon \sin \omega_2\xi),$$

in which one may take ω_2 to be the higher space frequency (radians per centimeter, say), present with the relative amplitude ϵ. In specializing the results, one may want to take ϵ small and ω_2 large, but no such approximations are involved in (38).

The summation on n is to range over positive integers for $m=0$. Otherwise, for $\omega_2>\omega_1$, m is to be positive and n is to range over both positive and negative integers. These values of m, n fall into five interesting categories, which are

1) Fundamental and harmonics of lower tone:

$$m = 0,\ n = 1, 2, \cdots$$

2) Fundamental of higher tone:

$$m = 1,\ n = 0$$

3) Upper modulation side tones on higher tone:

$$m = 1,\ n = 1, 2, \cdots$$

4) Lower modulation side tones on higher tone:

$$m = 1,\ n = -1, -2, \cdots$$

5) Harmonics of higher tone and their side tones:

$$m = 2, 3, \cdots,\ n = \pm 1, \pm 2, \cdots.$$

Selecting (2), for example, it is easy to see that the fundamental of the higher tone vanishes whenever

$$H_{1,0} = (2/\beta_2)J_0(\beta_2)J_1(\epsilon\beta_2) \tag{39}$$

vanishes. For $\epsilon \leq 1.5933$, this interesting phenomenon[13] occurs for the first time at the first null[14] of J_0, namely,

$$\beta_2 = 2.2048,$$

in agreement with the result from phase perturbation.[5]

[13] J. G. Woodward and E. C. Fox, "A study of tracking-angle errors in stereodisk recording," IEEE Trans. on Broadcast and Television Receivers, vol. BTR-9, pp. 48–55; May, 1963.

[14] E. Jahnke and F. Emde, "Tables of Functions," Dover Publications, Inc., New York, N. Y., p. 166; 1945.

Again, one may write, from 3)

$$H_{1,1} = 2J_1(\beta_2+\beta_1)J_1(\epsilon\beta_2+\epsilon\beta_1)/(\beta_2+\beta_1) \tag{40}$$

for the upper side tone, and

$$H_{1,-1} = -2J_1(\beta_2-\beta_1)J_1(\epsilon\beta_2-\epsilon\beta_1)/(\beta_2-\beta_1) \tag{41}$$

for the lower side tone, upon the application of (37). The first-order amplitude intermodulation index is

$$\bar{m} = (H_{1,1} + H_{1,-1})/H_{1,0}, \tag{42}$$

and the corresponding first-order phase intermodulation index is

$$\bar{\beta} = (H_{1,1} - H_{1,-1})/H_{1,0}. \tag{43}$$

The bar is used to denote the fact that these are not the usual definitions of these indexes, since, by taking only the first-order side tones into account, they neglect the fact that the modulating waveform is not a simple sinusoid. They do reduce, for $\epsilon \ll 1$ and $\beta_1<\beta_2\ll 1$, to the results previously derived by the phase perturbation method.

Phase crossmodulation (PXM)[5] happens only with tracking error and has no analog in tracing error. Let it be supposed that the signal $A \sin \omega_1\xi$ is mis-tracked in one mode of groove modulation, and the signal $\epsilon A \sin \omega_2\xi$ is properly tracked in the orthogonal mode. The two modes could be the conventional 45-45 ones,[15] the vertical-lateral ones, or any other orthogonal pair. The parametric equations are

$$x = \xi - kA \sin \omega_1\xi,$$
$$y = \epsilon A \sin \omega_2\xi.$$

The present method of analysis eliminates ξ to yield the Fourier series

$$y(x) = \epsilon A\beta_2\Sigma_n H_n \sin(\omega_2 + n\omega_1)x, \tag{44}$$

in which

$$H_n = J_n(\beta_2 + n\beta_1)/(\beta_2 + n\beta_1),$$

and the summation is to range over positive and negative n, with interpretations analogous to those for (38) except that the analog of (42) has no obvious meaning.

The series (35) converges for all x if $0 \leq \beta_1 \leq 1$, but its derivative,

$$y'(x) = (2/k)\Sigma_n J_n(n\beta_1) \cos n\omega_1 x,$$

fails to converge for $\beta_1 = 1$ and x an integral multiple of $2\pi/\omega_1$. This is as it should be, since it can be seen from (25) that the slope should be infinite, for $\beta_1=1$, at those points. Similar observations may be made for (38) and (44). These conditions correspond to a maximum-slope limitation for tracking and to a maximum-curvature limitation for tracing.

[15] C. C. Davis and J. G. Frayne, "The Westrex stereo disc system," Proc. IRE, vol. 46, pp. 1686–1693; October, 1958.

Contributors

Donald G. Burkhard was born in West New York, N. J. He attended the California Institute of Technology, Pasadena, and the University of California, Berkeley, receiving the A.B. degree in physics in 1941. He received the M.S. degree in 1947 and the Ph.D. degree in physics in 1950 from the University of Michigan, Ann Arbor.

He joined the staff of the University of Colorado, Boulder, in 1950. He is now a Professor of Physics at that institution. His primary research efforts have been in the field of molecular structure, microwave spectroscopy, and solid state physics.

Mr. Burkhard is a member of the following societies: American Physical Society, American Association of Physics Teachers, American Institute of Aeronautics and Astronautics, American Association for the Advancement of Science, Scientific Research Society of America, New York Academy of Science, American Institute of Radio Engineers, Colorado-Wyoming Academy of Science, Sigma Xi, and American Association of University Professors.

Marvin Camras (S'41–M'41–SM'47–F'52), for a photograph and biography, please see p. 98 of the May-June, 1963 issue of these Transactions.

❖

Duane H. Cooper, for a photograph and biography, please see p. 73 of the March-April, 1963 issue of these Transactions.

❖

Harumasa Ito was born in Tokyo, Japan, on June 30, 1933. He received the B.S. degree in electrical engineering in 1957 from the University of Tohoku, Sendai, Japan. He received the M.S. degree in physics in 1962 from the University of Colorado, Boulder. He is presently working for the Ph.D. degree in physics at the University of Colorado where he has been a teaching assistant since 1957.

Mr. Ito is an associate member of Sigma Xi, a member of American Physical Society and Electrical Communication Engineering Society of Japan.

C. B. Speedy (M'49) was born in Auckland, New Zealand, on April 13, 1927. He received the B.E. degree, with honors, in electrical engineering from the University of New Zealand, Christchurch, New Zealand, in 1948, and the Ph.D. degree from the University of Sydney, Australia, in 1952.

After a period with the Dominion Physical Laboratory, New Zealand, he took up a Research Fellowship at the Imperial College of Science and Technology, London, England. For several years he was Technical Director with the Gresham Lion Group Ltd. in England. He joined the University of New South Wales, Australia, in 1961 and was recently appointed to the second chair of Electrical Engineering. His work has been concerned mainly with electronic data processing systems, and at present he is closely associated with the University's post graduate work in the field of automatic control systems.

Dr. Speedy is a member of MIEE and AMIEE.